Research Square

Preprints are preliminary reports that have not undergone peer review.
They should not be considered conclusive, used to inform clinical practice,
or referenced by the media as validated information.

Urban Heat Island expansion in Khulna City of Bangladesh (1995-2025): Linking LULC change and Land Surface Temperature to heat-related health and economic risks

Halima Akter
University of Barisal
Dipok Chandra Nath
University of Barisal
Md. Abdur Rahman Bijoy
University of Barisal
Irteja Hasan
irteja07@gmail.com

University of Barisal
Md. Riajul Islam
University of Barisal
Hasan Shariar Shawron
University of Barisal
Musrat Mehjabin Asha
University of Barisal
Muhammad Iftekhar Uddin
University of Barisal
Esrat Jahan Papri
University of Barisal
Md Shafiqul Islam
EQMS Consulting Limited

Article

Keywords: Heatwave, Land Use/cover, Principal Component Analysis (PCA), Health Impact, Khulna City, Bangladesh

Posted Date: August 3rd, 2026

DOI: https://doi.org/10.21203/rs.3.rs-9960459/v1

License: This work is licensed under a Creative Commons Attribution 4.0 International License.
Read Full License

Additional Declarations: No competing interests reported.

Urban Heat Island expansion in Khulna City of Bangladesh (1995-2025): Linking LULC change and Land Surface Temperature to heat-related health and economic risks

Halima Akter[a], Dipok Chandra Nath[b], Md. Abdur Rahman Bijoy[c], Irteja Hasan[a]*, Md. Riajul Islam[a], Hasan Shariar Shawron[c], Musrat Mehjabin Asha[a], Muhammad Iftekhar Uddin[a], Esrat Jahan Papri[d] & Md Shafiqul Islam[e, f]

[a] Department of Coastal Studies and Disaster Management, University of Barishal, Barishal-8254, Bangladesh

[b] Department of Geology and Mining, University of Barishal, Barishal-8254, Bangladesh

[c] Department of Statistics and Data Science, University of Barishal, Barishal-8254, Bangladesh

[d] Department of Soil, Water and Environment, University of Barishal, Barishal-8254, Bangladesh

[e] EQMS Consulting Limited, Dhaka, Bangladesh

[f] GIS & RS Solution, Dhaka, Bangladesh

***Corresponding author:** Irteja Hasan (irteja07@gmail.com)

Rapid urbanization and climate change are intensifying urban heat stress in many developing countries, particularly in densely populated and climate-vulnerable regions. In Khulna City Corporation (KCC), Bangladesh, rapid land use and land cover (LULC) transformation has increased exposure to the Urban Heat Island (UHI) effect, posing growing threats to public health, livelihoods, and urban sustainability. However, the combined influence of urban expansion, thermal dynamics, and heatwave-induced socio-economic vulnerability remains insufficiently understood. The spatiotemporal relationship between LULC change, land surface temperature (LST), UHI intensity, and socio-economic vulnerability using Google Earth, statistical analyses, principal component analysis (PCA), and household survey data are presented. Vegetation cover shrank from 72.21% to 45.09% while built-up areas expanded from 10.12% to 32.16% from 1995 to 2025. LST over 40°C increased from 44% in 2015 to 67% in 2025. Correlation analysis showed a high positive association between LST and UHI intensity ($r \approx 0.99$) while NDVI was negatively correlated with LST, implying a cooling effect of vegetation. PCA showed LST, NDBI, and LULC were the most significant factors determining urban thermal variation. Survey results showed sleep disruption (36.7%) and heat-related discomfort (35.6%) were the most common impacts. Pregnant women (55.2%), elderly people (31.6%), and outdoor workers (27.5%) were identified as the most vulnerable groups. Heatwaves also reduced productivity and worsened water shortages (40%), food prices (23.8%), and power shortages. Results show that fast urban expansion and loss of green space are increasing heat exposure and socio-economic vulnerability in KCC. The study provides evidence to support climate-sensitive urban planning, green infrastructure development, and targeted adaptation strategies to improve urban resilience in fast-growing coastal cities.

Keywords: Heatwave, Land Use/cover, Principal Component Analysis (PCA), Health Impact, Khulna City, Bangladesh.

1 Introduction

Urban areas typically experience higher ambient temperatures than their suburban and rural counterparts. This occurrence, referred to as the 'Urban Heat Island'(UHI) Phenomenon, has been extensively documented in more than 400 cities around the globe (Santamouris, 2020). Urbanization is closely linked to changes in land use and land cover (LULC), which correspond to variations in land surface temperature (LST) and the intensity of the UHI phenomenon (Rahman et al., 2022a). It is directly related to heat waves (HW), which are defined as an extended period during which temperatures reach unusually high levels, often coupled with increased humidity (Mannan et al., 2022). Increased temperatures from climate change and UHI can lead to a rise in various diseases, severely threatening human health and life (Huang et al., 2020). In 2015, HW accounted for four of the ten deadliest natural disasters globally, with South Asian HW ranking as the third and fourth most lethal in terms of mortality (Nissan et al., 2017). In Bangladesh, the increasing frequency of HWs in other seasons, including pre-monsoon seasons (April-June), has been observed in recent years, indicating a significant relationship between HWs and dry conditions (Mannan et al., 2022). Urban environments further elevate the rate of warming in cities through the UHI effect, a phenomenon where the impervious materials of urban construction absorb, store, and release heat energy (Vargo et al., 2016). Increased heat is often linked to global warming and the potential impacts of a global temperature rise of 1° °C to 2° °C. In urban areas, temperatures can exceed those in rural surroundings by 8° °C to 10° °C. The implications of the UHI effect for resident health, comfort, and energy consumption during heat waves are significant but not yet fully understood (Van Der Hoeven & Wandl, 2015). The varying rates of warming highlight the urgent need to assess the health risks associated with HW, the focus of our study. Heatwave-related disasters result from complex interactions between global and local factors (Xu et al., 2025). Due to the impacts of climate change, HW's are becoming more intense. This phenomenon, combined with the effects of rapid urbanization, poses significant thermal risks for urban populations (Nadeem et al., 2022).

Identifying populations vulnerable to heat-related mortality and morbidity is essential for managing the public health risks of heat stress (Tran et al., 2020). Remotely sensed indices, including the Soil-Adjusted Vegetation Index (SAVI), Normalized Difference Building Index (NDBI), and Normalized Difference Drought Index (NDDI), have limitations in observing built-up and barren lands. These challenges arise from difficulties in correlating pixels to the spectral responses of diverse land use and land cover (LULC) types, such as water bodies, vegetation, and urban areas (Rahman et al., 2022a). Further research is crucial to enhance our knowledge of heatwaves in South Asian countries like Bangladesh, focusing on climate hazards, societal exposure, and population vulnerability (Nissan et al., 2017). In this case, Principal Component Analysis (PCA) involves a mathematical procedure to transform several correlated variables into a smaller number of uncorrelated variables to handle large datasets and also pinpoint major indicators by reducing dimensionality that contribute most to vulnerability ((Samsuddin et al., 2025), (Martinez Vale et al., 2008). To find links between daily emergency admissions and extreme health events, researchers use a hybrid methodology based on a heat wave recognition tool, multivariate analysis (PCA), and regression analysis.

(Telesca et al., 2018). PCA is frequently used to indicate heat vulnerability indices (HVIs), which are used to map populations that are susceptible to excessive heat (Conlon et al., 2020)

Changes in land cover impact thermal capacities, albedo coefficients, heat conductivity, and moisture levels, leading to local air and surface temperatures that may be several degrees higher than those in surrounding areas. As urban areas expand, the implications of UHI become more pronounced, affecting both human populations and the environment in urban settings (Mirzaei et al., 2020). Bangladesh is highly vulnerable to environmental stressors, particularly HW's (Adnan et al., 2024). We selected the area of Khulna because of its increasing urbanization and lack of consideration of it as a high heat wave-induced area (Rahman et al., 2022a). Khulna, the third-largest industrial city in Bangladesh, is experiencing significant urban expansion, which is contributing to rising summer temperatures. Therefore, conducting a trend analysis of HW's is crucial to understanding heat impacts and fostering sustainable development (Nureen et al. 2024). Research has shown a link between heatwaves and increased morbidity and mortality. For example, the 2003 HW in Western Europe led to over 70,000 deaths (Sestito et al., 2025). UHIs are growing in intensity and frequency, posing health risks and worsening socioeconomic disparities among vulnerable populations. A study was conducted using a mixed-methods approach to examine the effects of heat waves on public health and socioeconomic inequalities, as well as the adaptive strategies employed by households in Rajshahi, Bangladesh, a region affected by rapid urbanization and Urban Heat Island (UHI) effects (Hossain et al., 2024). This type of study lacked coverage of the Khulna city area, so we assessed the data for Khulna city and analyzed the impact of HWs. This study analyzes HWs, including correlation and regression analysis between factors, to assess the health and economic impacts of heatwaves. It also explores LULC, LST, and UHI in Khulna city between 1995 and 2025, examining their correlations. The UHI effect is a key concern associated with urbanization, as it raises temperatures that can exacerbate health risks from thermal stress. Addressing it is crucial for public health (Tan et al., 2010). To identify the elements causing heat stress, PCA can be used, which can be preceded by data pretreatment, including standardising numerical variables and encoding categorical variables(Muhamad et al., 2024). High temperatures can cause discomfort and lead to serious health issues, including heat-related illnesses and fatalities (Dong et al., 2014). The situation poses serious health risks, undermines adaptability, and impacts water safety and agriculture, while exacerbating droughts. HW's can increase agitation and mental health issues, escalating public disorder risks (Mannan et al., 2022). The study calls for targeted interventions for low-income households and vulnerable groups during HW's (Hossain et al., 2024). Age and health conditions impact the ability to adapt to high temperatures. Older adults, particularly those over 65 years old, and infants under one year old face higher risks during heat waves.

Additionally, lower-income populations often experience more severe effects due to limited access to green spaces and elevated urban temperatures (Vargo et al., 2016). This work includes a thorough approach to HVI preparation, which is built using data taken from census tracts and remote sensing data evaluated using PCA (Kotharkar et al., 2022). We conducted a survey to identify the exact vulnerable individuals and areas for improvement. Urban residents struggle to respond to extreme heat due to limited knowledge of adaptation strategies (Hossain

et al., 2024). Thus, a study on urbanization's impact on UHI intensity is critical for Bangladesh, a densely populated, resource-limited country (Rahman et al., 2022a). Heat-related deaths can be prevented with early warning systems in developed cities (Nissan et al., 2017). Integrating the UHI effect at the sub-district level can aid effective urban planning and disaster preparedness (W. Dong et al., 2014). Recent research has enhanced our understanding of urban overheating and UHI effects through the use of integrated assessment frameworks. Although data sources like remote sensing and meteorological records enhance HW risk evaluations, significant methodological gaps remain (Xu et al., 2025). The methodological approaches taken for bridging this research gap and achieving the objectives of this study are: (1) spatial and temporal variability assessment of temperature and land use dynamics in Khulna City using satellite-derived indicators such as LULC, LST, NDVI and NDBI; (2) the relationships between these variables were quantified using correlation and regression analyses to assess their combined impact on the intensity of the Urban Heat Island (UHI) effect; (3) the evaluation of the effectiveness of PCA of heatwave for mapping the spatial footprint and temporal trends. PC1 captures the dominant, large-scale spatial pattern of the heat wave and PC2 and PC3 often capture secondary effects, like localized coastal-inland temperature contrasts or seasonal shifts; (4) the impact of heat exposure on public health and economic outcomes was assessed by analyzing the differences in health conditions, healthcare access, and productivity of the urban population; and (5) the environmental and socio-economic findings were integrated to provide a comprehensive understanding of how urban heat interacts with land surface characteristics and impacts human well-being. This integrated methodological framework is expected to yield evidence-based insights to inform future research and guide policy interventions aimed at mitigating the impacts of urban heat in rapidly growing cities.

2 Materials and methods

2.1 Study Area

Khulna City Corporation (KCC) is located in southwestern Bangladesh (Jahan et al., 2022). As the third-largest city in the country, Khulna City has a Population of approximately 0.8 million. KCC is situated near the Sundarbans, the largest mangrove forest, which influences its climate and ecology (Haque et al., 2020). Khulna City Corporation covers an area of 64.76 square kilometres. Population density is approximately 0.016268 million people per square kilometre(Ara, 2022). In December 1984, Khulna was likewise promoted to city corporation status (Fig. 1). Historical elements, such as Khulna's establishment as a divisional headquarters and the development of Mongla Port, have influenced the city's growth (Hasan et al., 2022). Due to migration and economic development, KCC's built-up areas increased by 6.76% between 2010 and 2020, accelerating urban expansion (Alam et al., 2023). Its location along the Rupsha and Bhairab rivers, and its proximity to the Sundarbans mangrove forest, contribute to ecological complexity and affect regional climate patterns. Due to inadequate drainage systems, the city receives excessive rainfall, which frequently causes waterlogging, particularly during the rainy season. situated in Bangladesh's low-lying region (Fahim et al., 2024).

2.2 Data and Methods

Satellite images from Landsat-5 and Landsat-8 for the years 1995, 2005, 2015, and 2025 were downloaded during the winter season to ensure consistent seasonal conditions for analysis. The winter period was selected because of its significant impact on Urban Heat Island (UHI) intensity, which varies with satellite overpass time across districts. Additionally, the effects of UHI on energy consumption and health differ between summer and winter, underscoring the importance of the winter season for understanding these dynamics. Furthermore, urban cooling measures may affect UHI intensity differently in winter, making this season important for evaluating their effectiveness. The images were preprocessed and analysed in ArcGIS 10.8 to calculate Land Surface Temperature (LST) and NDVI, and to perform LULC classification, as outlined in the study's flowchart in Fig. 2.

2.3 Data Acquisition and Pre-Processing

We obtained Landsat-5 (1995, 2005) and Landsat-8 (2015, 2025) images from the Google Earth Engine website (https://earthengine) to classify LULC, compute NDVI and LST, and identify changes in UHI. This site was also used to collect digital elevation data for the study area. Table 1 provides information on the path, row, and acquisition dates. All images have a 30m spatial resolution, except for Landsat-5 band 6, which has a 120m resolution. We also used this source to obtain digital elevation data for the research area. Table 2 provides a more detailed view of the path, row, and acquisition dates. The spatial resolution of all images is 30 m, except for Landsat-5 band 6 (120 m) and Landsat-8 bands 10 and 11. To keep the research area free of clouds, all images were taken when the cloud cover was between 0% and 5%. We used ArcMap 10.8 to classify LULC, determine LST and NDVI, and calculate UHI in a table. 1.

2.4 Classification of LULC

We utilized Landsat-5 and Landsat-8 pictures to sort LULC. We utilized the maximum likelihood supervised classification (MLSC) technique to classify LULC using training sample areas (Al Kafy et al., 2020). The photographs were put into four groups: bare ground, built-up area, vegetation, and water body. For each class, about 40 to 50 sample locations were collected to make the LULC map. The description of land cover categories is in the table. 2.

2.5 Accuracy Assessment of LULC

The accuracy assessment process evaluates the accuracy of computer-generated maps by presenting descriptive statistics that compare the classifications with the ground truth. Approximately 200 to 220 locations were designated as ground observation points to verify the accuracy of the LULC map in 1995, 2005, 2015, and 2025 in KCC. Google Earth Engine was used to verify those points. Computer-classified maps and ground inspections helped determine four classes: barren terrain, built-up area, vegetated water body, and body. The error matrix was used to determine overall accuracy, user accuracy, producer accuracy, and the kappa coefficient. The conventional kappa coefficient was used to measure agreement. When the

kappa coefficient exceeds 0.75, accuracy is considered satisfactory. The findings of this investigation demonstrate that the accuracy was over 0.75. The accuracy of all the users, producers, and kappa coefficients is determined, and the results are shown in the table. 3.

2.6 NDVI Derivation

The NDVI is a standard way to find out how much green biomass is in an area (SINGH, 1989). The NDVI approach has been widely utilized to identify various plant types and areas devoid of plants (Matsushita et al., 2007). It is a ratio of the R (red) and NIR (near-infrared) readings, which are utilized to determine it. We used the NDVI to examine the relationship between changes in built-up and vegetated areas and LST. It is advantageous for our research to determine plant density and monitor changes in their health. The normalized reflectance ratio is used to determine band ratios that indicate vegetation density. It does this by examining the visible (Red) and near-infrared (NIR) sections of the electromagnetic spectrum. The values given can range from -1 to +1, indicating they can be either negative or positive. This shows that the distribution is symmetric around zero. The positive (+) values indicate a high abundance of flora, whereas the negative (-) values signify areas with low flora abundance, such as water bodies and residential areas. We used an ArcGIS spatial analysis tool (a raster calculator) to figure out the NDVI matrices for the years 1995–2025, following the Equation:

$$NDVI = \frac{(NIR - RED)}{(NIR + RED)} \tag{2.1}$$

where Landsat 4–7,

$$NDVI = \frac{Band4 - Band3}{Band4 + Band3} \tag{2.2}$$

Additionally, Landsat-8,

$$NDVI = \frac{Band5 - Band4}{Band5 + Band4} \tag{2.3}$$

2.7 LST Derivation for Landsat-5

For several processes, thermal band six was employed to figure out the LST for Landsat-5 satellite photos (Fatemi & Narangifard, 2019). This can be carried out in three steps:
1st Step: Change the digital number (DN) to Radiance (L_λ):

$$L_\lambda(TOA) = \left(\frac{L_{max_\lambda} - L_{min_\lambda}}{Q_{cal(max)} - Q_{cal(min)}}\right)\left(Q_{cal} - Q_{cal(min)}\right) + L_{min_\lambda} \tag{2.4}$$

2nd Step: Convert TOA Radiance to Brightness Temperature (BT):

$$L_{BT} = \left(\frac{K_2}{Ln\left(\frac{K_1}{L_1} + 1\right)}\right) \tag{2.5}$$

3rd Step: Correct for Surface Emissivity (E):

$$LST = \left(\frac{T_{BT}}{1 + \left(\frac{T_{BT}}{\rho}\right) \ln(E)} \right) \quad (2.6)$$

4th Step: Calculate Surface Emissivity (E):

a. Calculate NDVI:

$$NDVI = \left(\frac{NIR - RED}{NIR + RED}\right) \quad (2.7)$$

b. Use NDVI to estimate emissivity:

- E = 0.97 for dense vegetation (NDVI > 0.7)
- E = 0.92 for bare soil (NDVI < 0.2)
- Linearly interpolate for 0.2 ≤ NDVI ≤ 0.7

2.8 LST Derivation for Landsat-8

Thermal band 10 was utilized to get the temperature of the ground surface for Landsat-8 (He et al., 2019). This can be done in six phases.

Convert DN to Radiance: Use the following formula to convert digital numbers (DN) from the thermal band (Band 10) into spectral radiance:

$$L_\lambda = ML \times DN + AL \quad (2.8)$$

After changing the spectral radiance in Step 2, it needs to be changed to the atmospheric temperature brightness (Gutman et al., 2013).

$$BT = \frac{K_2}{\ln\left(\frac{K_1}{L_\lambda} + 1\right)} - 273.15 \quad (2.9)$$

Step 3 involves calculating NDVI, a prerequisite for determining LST in Landsat-8 (Gutman et al., 2013).

Step 4 is the calculation of the proportion of vegetation using the maximum and minimum NDVI,

$$P_v = \left(\frac{NDVI - NDVI_{min}}{NDVI_{max} - NDVI_{min}}\right)^2 \quad (2.11)$$

Step 5 is the calculation of land surface emissivity using P_v (Avdan & Jovanovska, 2016)

$$\varepsilon = 0.004 \times P_v + 0.986 \quad (2.12)$$

In step 6, finally, use the following formula to convert the brightness temperature to LST

$$LST = \frac{BT}{1 + \left(\frac{\lambda \times BT}{\rho}\right) \ln(\varepsilon)} \quad (2.13)$$

2.9 Statistical Analysis Method

As the population of the Khulna City Area was large and the exact number was not available, we used the Cochran equation. The Equation is widely used for surveying a large, unknown population. For an unknown population size, the formula is:

$$\eta_0 = \frac{Z^2.p.q}{e^2} \quad (2.14)$$

where:

- n_0 = initial sample size (for an infinite or unknown population)
- Z = Z-value (based on the desired confidence level; e.g., 1.96 for 95% confidence)
- p = estimated proportion of the population having the attribute of interest (if unknown, use 0.5 for maximum variability)
- q = 1 − p
- e = margin of error (in decimal form; e.g., 0.05 for 5%)

2.10 Estimation of UHI

People commonly talk about UHI as the contrast between cities and the countryside (Hu et al., 2019). The difference can also be defined by measuring how urban surfaces affect climate change in their own areas and in the surrounding areas (Hu et al., 2019). To determine the UHI, the value of land surface temperature was utilized (Rahman et al., 2022).

$$UHI = \frac{T - T_m}{T_{sd}} \tag{2.15}$$

2.11 Principal Component Analysis (PCA)

Principal Component Analysis (PCA) was applied in this study to identify dominant spatial and spectral patterns among the multi-dimensional geospatial indices derived from Landsat 8/9 imagery, such as NDVI, LST, UHI, NDBI, and LULC classification outputs. Due to the inherent intercorrelation among these indices, particularly between LST and UHI, and between NDBI and LULC urban classes, PCA was employed to reduce redundancy, extract orthogonal components, and reveal the underlying environmental gradients governing urban surface dynamics within the study area. Before PCA computation, all five input variables (NDVI, LST, UHI, NDBI, and LULC) are standardized to have a mean = 0 and a variance = 1, z-score normalization using equation 01. This pre-processing step is essential in remote sensing applications to ensure that variables with differing measurement scales and magnitudes using equation 01

$$Z = \frac{X-\mu}{\sigma} \text{.....01}$$

where X is the original variable, μ is the mean, and σ is the standard deviation.

Secondly, the covariance matrix Σ is computed from standardized data using equation 02

$$\Sigma = \frac{1}{n-1}\sum_{i=1}^{n} (x^{(i)} - \bar{x})(x^{(i)} - \bar{x})^T \text{.....02}$$

where $\bar{x}$ is the mean vector and n is the number of data vectors.

Principal components are eigenvectors of the covariance matrix, satisfying using equation 03

$$\Sigma v = \lambda v \text{.....03}$$

where v is the eigenvector (principal component direction) and λ is the corresponding eigenvalue.

The proportion of total variance explained by the k-th principal component:

306 $$\text{Var}_k = \frac{\lambda_k}{\sum_{i=1}^{m} \lambda_i} \ldots\ldots\ldots\ldots\ldots\ldots 04$$

307 where λ_k is the eigenvalue of component k and m is the total number of variables.

308 The cumulative variance for the first S components:

309 $$\text{Cumulative Var} = \frac{\sum_{i=1}^{S} \lambda_i}{\sum_{i=1}^{M} \lambda_i} > R \ldots\ldots\ldots\ldots\ldots\ldots 04$$

310 where R is typically ≥ 0.60 (or 0.90 for stringent criteria).

311

312 PCA was performed using the *scikit-learn* library (v1.4) in Python 3.4. The number of principal
313 components (PCs) to retain was determined using a cumulative explained variance threshold
314 of 80%, meaning that only those components whose combined explained variance reached or
315 exceeded this threshold were retained for further analysis. Component loadings were examined
316 to interpret the physical and environmental significance of each retained principal component.
317 Loadings represent the correlation between each original variable and the derived component;
318 high absolute loading values (positive or negative) indicate a strong association between that
319 variable and the corresponding component axis. For instance, a component exhibiting strong
320 positive loadings on NDBI and LST alongside a strong negative loading on NDVI is interpreted
321 as representing the urban heat-vegetation contrast gradient, a well-documented phenomenon in
322 urban thermal remote sensing studies. LULC class distributions were cross-referenced with
323 component score maps to validate the spatial correspondence between derived components and
324 observed land surface conditions.

325 ## 2.12 Statistical Analysis

326 Bivariate distribution analyses were conducted to examine how various reported health and
327 economic consequences of heatwaves are distributed across the high and low impact groups
328 (Agresti, 2018).

329 ### **2.12.1** Construction of Outcome Indices

330 Two composite scores were developed to quantify heatwave vulnerability (Fayers et al., 2005):

331 - **Health Impact Score (HIS):** Represents the cumulative count of reported physical and
332 psychological health issues during heatwaves, including sleep disruption, physical
333 discomfort, stress, cognitive impairment, anxiety, PTSD, social isolation, economic-related
334 distress, headache, heatstroke, dehydration, and heat exhaustion (Niu et al.; Rathi et al.,
335 2022).
336 - **Economic Impact Score (EIS):** Captures reported economic hardships and access
337 challenges, including job loss, income reduction, forced business changes, homelessness,
338 disruptions to farming and food supply chains, water and healthcare scarcity, increased
339 commodity prices, power shortages, and overall living cost increases (García-León et al.,
340 2021).

341 Each response item under the health and economic domains was recoded as a binary indicator
342 (Hosmer et al., 2013):

$$x_{ij} = \begin{cases} 1, & \text{if respondent } i \text{ selected response } j \\ 0, & \text{otherwise} \end{cases} \quad \text{for } j = 1,2,\dots,K \tag{2.16}$$

For each respondent i, The total score is calculated as:

$$\text{Impact Score}_{\,i} = \sum_{j=1}^{K} x_{ij} \tag{2.17}$$

where K is the number of relevant items (12 for HIS and 16 for EIS).

These scores were then dichotomized at their respective median values to construct binary outcomes for regression analysis (Altman & Royston, 2006):

$$Y_i = \begin{cases} 1, & \text{if Impact Score}_{\,i} > \text{Median} \quad \text{(High impact)} \\ 0, & \text{if Impact Score}_{\,i} \leq \text{Median} \quad \text{(Low impact)} \end{cases} \tag{2.18}$$

Thus, the outcome Y_i reflects whether an individual experienced high or low impact.

2.12.2 Modeling High Impact Using the Binary Logistic Regression Model

We categorized impact scores as high or low and applied binary logistic regression because it effectively models the probability of categorical outcomes and estimates the influence of multiple predictors on the effects of severe heatwaves (Hosmer et al., 2013; Menard, 2002).

The general form of the model is:

$$\log\left(\frac{P(Y_i = 1)}{1 - P(Y_i = 1)}\right) = \beta_0 + \sum_{j=1}^{p} \beta_j X_{ij} \tag{2.19}$$

where, Y_i: binary indicator ($1 =$ high impact, $0 =$ low impact), X_{ij}: independent variables, β_j: model coefficients for predictors. Model estimation was performed via maximum likelihood estimation (MLE) (Ananth & Kleinbaum, 1997). The regression coefficients β_j were interpreted in terms of odds ratios: $OR_j = e^{\beta_j}$ (Bland & Altman, 2000).

2.12.3 Correlation Analysis

To evaluate the linear relationships among the selected indicators for 1995, 2005, 2016, and 2025, the Pearson correlation coefficient was used.

For two variables X and Y, The coefficient is:

$$r_{XY} = \frac{\text{Cov}(X,Y)}{\sigma_X \sigma_Y} = \frac{\sum_{i=1}^{n} (x_i - \bar{x})(y_i - \bar{y})}{\sqrt{\sum_{i=1}^{n} (x_i - \bar{x})^2}\sqrt{\sum_{i=1}^{n} (y_i - \bar{y})^2}} \tag{2.20}$$

where:

- $x_i, y_i =$ observed values of two variables,
- $\bar{x}, \bar{y} =$ their means,
- $\sigma_X, \sigma_Y =$ standard deviations,
- $n =$ number of complete observations.

The results for each year are presented in the form of a correlation matrix:

$$R = \begin{bmatrix} 1 & r_{12} & r_{13} & r_{14} \\ r_{21} & 1 & r_{23} & r_{24} \\ r_{31} & r_{32} & 1 & r_{34} \\ r_{41} & r_{42} & r_{43} & 1 \end{bmatrix} \tag{2.21}$$

This symmetric matrix summarizes all pairwise correlations among the variables, with diagonal elements equal to 1 and off-diagonal elements representing the correlation coefficients.

2.13. Ethical considerations

Ethical approval for this study was granted by the Department of Coastal Studies and Disaster Management, University of Barishal, Bangladesh (Approval No. BU/SDS/Research/2025/40). Prior to participation, all respondents were thoroughly briefed on the study's aims, procedures, potential risks, and anticipated benefits, and written informed consent was obtained from each individual. Where participants were minors or otherwise unable to provide consent independently, written consent was secured from their legal guardians. Throughout the study, strict measures were maintained to protect the confidentiality and anonymity of all participants.

3 Results

3.1 Land use and land cover changes

From 1995 to 2025, the land use and land cover (LULC) in the Khulna City Corporation (KCC) area underwent significant changes. The distribution of land types underwent the most significant changes. The city's rapid growth has been the most significant change, resulting in smaller areas with green spaces and water features. In 1995, water bodies made up 7.05% of the KCC area. This number dropped to 6.87% by 2025, indicating a decline in the number of bodies of water over time. Urban growth has encroached on riverbanks and other water-rich areas in the city, leading to this reduction. In 1995, plants comprised 72.21% of the land, but by 2025, this will decrease to 45.09%. This drop of almost 27% indicates that stress levels are rising due to urbanization, industrialization, and agricultural growth, particularly in areas such as Khulna. Cities accounted for 10.12% of the KCC area in 1995. They will be 32.16% of the total by 2025. The city's central regions and surrounding districts are where most people are moving. Khulna City has experienced significant growth over the past 20 years. Cities have grown most in areas previously rural or semi-urban. The expansion of built-up areas in Khulna indicates that the city is shifting its focus from commercial and industrial areas to meet the growing demand for housing and infrastructure. Today, there is much less unoccupied land, as more and more land is pressed into service for homes, urban infrastructure, and the like, rather than being left fallow or used for farming. In 1995, 10.62 % of the land was still vacant. This percentage is expected to go down to 1.88% by 2025. The decrease in vacant land correlates with the city’s continuing urban sprawl, where homes, businesses, and infrastructure are being built on previously unoccupied land. The city is expanding its boundaries as the population grows, indicating the change of open land to developed urban land. This is summarized from Fig. 3.

3.2 Land use and land cover changes analysis

Land-use and Land-Cover change in Khulna City clearly tells the story of continuous urban growth over the last three decades. In 1995, the city was predominantly green with vegetation covering some 72% of the total area. Built-up land was some 10%, while water bodies and bare land were about 7% and 10% respectively. This balance had begun to shift by 2005. Vegetation had dropped to just under 60%, a loss of some 12 percentage points in only a decade, but urban land had rapidly expanded to around 25%. Water bodies had grown slightly to around 10%,

and bare land had shrunk to just under 3%, indicating that open spaces were being taken up into development. This trend continued in 2015, with vegetation falling to around 58% and urban areas rising to around 33%. Water bodies were still limited to about 5%, and bare land was very low, indicating a maturing urban landscape with little undeveloped space left. By 2025, the transformation became most apparent. Urban land rose to about 46%, slightly surpassing vegetation, which declined to around 45%. Over the entire period, vegetation decreased by nearly 27 percentage points, and urban land increased by about 36 percentage points. These changes broadly show the large and continuing conversion of natural and open land to built-up land in Khulna City and indicate the extent of urbanization and its likely environmental impacts in Fig. 4.

3.3 Land surface temperature change (LST)

Fig. 5 shows that in 1995, the Land Surface Temperature (LST) of Khulna city was mostly below 25°C to 30°C; hence, most of the areas were relatively moderate in terms of surface temperature. The western and southwestern sections remained relatively cooler with temperatures mostly below 30°C, while slightly higher values were observed in the central and eastern sections. In 2005, the LST range was increased to about 25°C–35°C, which was an overall increase of about 3°C compared to 1995, with higher temperature being recorded in the eastern and northeastern parts of the city, which was mostly in the range of 29.9°C and 35.7°C, while the western vegetated areas remained relatively cooler, mostly in the range of 25–30°C. In 2015, there was another increase in LST with temperatures ranging from about 25.7 °C to 39 °C, showing an increase of about 3.3 °C from 2005. High temperature zones (35–40 °C) significantly expanded over the eastern and northeastern built-up areas, where LST values consistently achieved their highest levels. The western parts of the city with vegetation cover remained relatively cooler with temperatures generally less than 31.1 °C. The northern areas showed a narrow temperature range, mostly between 27.6 °C and 31.1 °C. By the end of the study period in 2025, the maximum LST reached about 42 °C, representing a total increase of about 7–8 °C from the mid-1990s. Minimum temperatures also increased noticeably over time, indicating an overall warming of the city surface. High and very high LST classes (40–45°C and >45°C) became widespread, particularly in the eastern and northeastern urbanized zones, while lower-temperature classes were restricted to pockets in the western region. In general, the spatial–temporal patterns clearly show a steady increase in surface temperature over Khulna City, with the highest values consistently recorded in the densely built-up areas.

3.4 Normalized Difference Vegetation Index (NDVI)

The spatial-temporal distribution of Normalized Difference Vegetation Index (NDVI) in the study area for the years 1995, 2005, 2015, and 2025 is presented in Fig. 6. NDVI showed high temporal variability, with vegetation cover and health changes over the last 30 years. The NDVI values were between approximately 0.09 and 0.60 in 1995, with sparse or non-vegetated surfaces mainly in the south and peripheral areas. In 2005, a slight improvement in NDVI values was observed, with a maximum value of about 0.65 and a larger share of the region falling into the moderate to high NDVI range, especially in the central and northern parts of the region. The NDVI map of 2015 indicated a relatively stable pattern of vegetation cover

with values from 0.09 to 0.66. Green vegetation was still the most common land cover, but some low NDVI values persisted, pointing to localized vegetation stress or land-use changes. The NDVI map for 2025, however, showed a marked increase in the density and vigor of the vegetation, with the maximum NDVI value reaching around 0.74. The wider range (down to 0.19) also indicates increased heterogeneity, possibly related to urban expansion, water bodies, or exposed soil.

3.5 Normalized Difference Built-up Index (NDBI)

The NDBI maps from Khulna City Corporation show a significant increase in urbanization from 1995 to 2025, as analysed in Fig. 7. The numbers accompanying the maps indicate the size of the built-up areas. The NDBI values from 1995, ranging from -0.54 to 0.22, indicated minimal urbanization, with the landscape predominantly open spaces and vegetation. During this time, there are a few built-up areas, which are mostly limited to a small area of focus. The NDBI range changed slightly from -0.52 to 0.24 by 2005, indicating that urban areas were growing at a moderate rate, particularly in the City Centre. Although the growth of built-up areas was still relatively small compared to later years, it was evident. The trend of urbanization was stronger in 2015, when NDBI values ranged from -0.64 to 0.29. This has become increasingly common in densely populated areas, particularly in the central and southern parts of Khulna. Urban sprawl led to urban areas encroaching on open spaces and natural vegetation. The 2025 predicted map indicates that cities will experience growth, with NDBI values ranging from -0.76 to 0.33. Urban growth is a common phenomenon, particularly along major highways and urban corridors. We believe that built-up areas will occupy a significant portion of the city, indicating that urbanization is still progressing rapidly. These numbers indicate that the city is continually expanding, making green spaces increasingly scarce.

3.6 Spatiotemporal dynamics of Urban Heat Island (UHI) intensity

Figure 8 presents the spatial distribution and temporal variation of Urban Heat Island (UHI) intensity in the study area for the years 1995, 2005, 2015, and 2025. The UHI values exhibit substantial spatial heterogeneity and a clear temporal evolution over the 30 years. In 1995, UHI intensity ranged from approximately −9.36 to 11.8, with relatively moderate heat accumulation observed in localized pockets, while cooler zones were widely distributed across vegetated and peripheral areas. By 2005, the overall UHI intensity slightly declined in magnitude (−6.95 to 11.49), suggesting a temporary moderation of surface heat, particularly in northern and central regions. The 2015 UHI map indicates a renewed increase in heat intensity, with maximum values reaching approximately 12.05 and a wider spatial spread of moderate-to-high UHI zones, especially in the southern and central parts of the study area. Cooler patches persisted but became more fragmented, indicating increasing thermal heterogeneity. In contrast, the 2025 scenario demonstrates a pronounced intensification of the UHI effect, with maximum values rising sharply to about 14.67. Large contiguous areas exhibit high UHI intensity, while extreme negative values (down to −37.87) suggest strong thermal contrasts, possibly associated with water bodies or remaining vegetated areas. This pattern reflects a significant escalation of surface heat stress and spatial polarization between hot and cool zones.

3.7 Temporal variation of Urban Heat Island (UHI) statistics

The temporal changes in maximum, minimum, and mean Urban Heat Island (UHI) values for the years 1995, 2005, 2016, and 2025 are presented here. The results show a consistent increase in maximum UHI intensity over time, rising from approximately 12 in 1995 to around 15 in 2025, indicating a progressive intensification of surface heat in the study area. Conversely, minimum UHI values exhibit increasingly hostile extremes, particularly in 2025, when the minimum drops sharply to nearly −38. This reflects growing thermal contrasts between hot built-up areas and cooler surfaces such as water bodies or vegetated zones. The mean UHI values remain relatively close to zero across all years, suggesting that while average conditions appear stable, spatial variability and extremes have intensified significantly in Fig. 9.

3.8 Correlation Between Land Use Indicators and Urban Heat Intensity

Results from the study show in Fig. 10 a significant impact of land use change on the thermal environment of the city over time. The analysis of the satellite-derived data from 1995-2025 revealed the cooling effect of the vegetation cover as indicated by NDVI on the urban areas. The relationship between NDVI and LST was weakly positive in 1995 (R = 0.27) with little cooling. In 2005 (R = -0.25), 2015 (R = -0.21), and 2025 (R = -0.14), the relationship was negative, showing that areas with higher vegetation cover had relatively lower surface temperatures. However, the negative correlation weakened (approximately 44% reduction from 2005–2025), indicating a decrease in the cooling capacity of vegetation due to extensive loss of green cover.

In contrast, built-up areas show a strong warming effect. The correlation between NDBI and LST increased sharply from almost no relationship in 1995 (R = 0.01) to a strong positive association in 2005 (R = 0.73), 2015 (R = 0.77), and 2025 (R = 0.74). This represents an increase of more than 70% in correlation strength after 1995, confirming that impervious surfaces such as roads and buildings are major contributors to rising surface temperatures. These findings indicate the expansion of built-up area as the main contributing factor for urban heat in recent decades. In previous years, the correlation between Urban Heat Island (UHI) intensity and LST was remarkably strong, with correlation coefficients of R = 0.99 in both 1995 and 2005, and nearly perfect in 2015 (R = 1.00). In 2025, the relationship was weakened (R = −0.19), but the change indicates an increase in spatial heterogeneity of urban development rather than a reduction of heat stress, because areas of intense urbanization still have higher temperatures, but their heat distribution has become more uneven across the city.

3.9 Principal Component Analysis (PCA)

To reduce the dimensions of the dataset and extract the major factors influencing the characteristics of heatwaves, Principal Component Analysis (PCA) was employed.

3.9.1 Inter-band Correlation Analysis of PCA

To investigate the relationships between Land Surface Temperature (LST), Urban Heat Island intensity (UHI), Land Use/Land Cover (LULC), Normalized Difference Vegetation Index (NDVI), and Normalized Difference Built-up Index (NDBI), Pearson’s correlation analysis

was carried out (Figure 11). The results show a high positive correlation between LST and NDBI (r = 0.742), indicating that urbanized areas with a high level of built-up intensity are associated with higher surface temperatures. In parallel, LST was strongly positively correlated with LULC (r = 0.656), indicating that changes in land use patterns have a significant impact on thermal conditions. There was a weak negative correlation between LST and NDVI (r = -0.146), which indicates that the vegetation cover helps to cool down the temperature, but the relation is weak. The correlation between LST and UHI (r = -0.190) was also weak and inverse. The explanatory variables showed a strong positive correlation between LULC and NDBI (r = 0.726), which indicates the strong association between urban expansion and built-up land characteristics. NDVI had negative correlations with LULC (r = −0.128) and NDBI (r = −0.195), which means that vegetation cover generally decreases with urban development. UHI and NDVI exhibited positive correlation with moderate strength (r=0.300), and UHI had very weak negative relationships with LULC (r=-0.077) and NDBI (r=-0.056). In brief, the correlation matrix indicates that the factors related to urbanization (LULC and NDBI) are the primary causes of the upward trend of land surface temperature, while the vegetation cover (NDVI) acts to reduce thermal intensity. The strongest correlations were observed between LST–NDBI (r = 0.742) and LULC–NDBI (r = 0.726), emphasizing the significant impact of the expansion of built-up land on the urban thermal environment.

3.9.2 Principal Component Analysis (PCA) Biplots Showing Relationships Among UHI, NDVI, LST, and NDBI (PC1–PC2 and PC2–PC3)

Components with eigenvalues >1 were identified as important. PCA analysis identified two principal components, PC1 (LST, NDBI, LULC) and PC2 (NDVI, UHI), which explained 50.10% and 24.37% of the total variance, respectively. The two components jointly explained 74.48% of the cumulative variance. The cumulative variance would increase to 88.8% with the inclusion of PC3, but its eigenvalue suggested a relatively lower contribution in Figure 13.
The PCA biplot of PC1 vs PC2 indicates that LST, NDBI, and LULC are closely clustered and are the major factors contributing to heatwave intensity, suggesting that increases in surface temperature, urbanization, and land use change exacerbate heat stress conditions. NDVI and UHI in PC2 are negatively correlated with the major factors of heatwave generation, suggesting that the increase of vegetation cover can mitigate heat stress. In figure 12, the PC2 versus PC3 biplot also shows the inverse relationship between NDVI and UHI, i.e., the higher the density of vegetation, the lower the intensity of urban heat. LST, NDBI, and LULC are separated together, indicating a small direct correlation with the NDVI–UHI relationship. Overall, the PCA results highlight the great importance of vegetation in reducing urban heat effects, while increasing the extent of built-up land and surface temperatures are the main contributors to heatwave intensity.

3.10 Health and Economic Impacts of Heatwave

A survey was conducted among 400 randomly selected individuals in the Khulna region to assess the impact of heatwaves on health and socio-economic effects. The collected data were analyzed through Bivariate table interpretation.

3.10.1 Health Impacts of Heatwaves

According to a bivariate analysis based on 400 survey participants from the Khulna region, heatwaves have numerous detrimental effects on people's physical and mental health. In the survey, participants could choose multiple options (if applicable), and the results showed that many had experienced more than one symptom simultaneously, suggesting that heatwaves put the human body under combined physical, physiological, and environmental stress.

3.10.1.1 Physical Health Impacts

The analysis revealed that many respondents experienced physical discomfort. Here, 34 respondents experienced both low- and high-effect categories. However, among those with sleep disruption, 34 people experienced a high effect, while 28 experienced a low effect. This occurs because high ambient temperatures interfere with the body's thermoregulation, making it difficult for people to maintain a healthy body temperature while sleeping. The body is unable to adequately cool down at night, disrupting deep sleep cycles and leading to weariness and irritability. Additionally, the survey demonstrated that 23 people experienced a high effect on increased stress, while 19 reported a low effect. Nevertheless, only 4 respondents reported a strong effect, and 10 reported a low effect on cognitive impairment. This may be due to prolonged exposure to heat, which increases body temperature and can lead to dehydration and reduced cerebral blood flow.

3.10.1.2 Indirect Psychological Impacts

The survey also demonstrated a significant mental health dimension. It has been observed that anxiety and depression were the prominent issues during the heatwave, which was experienced by 44 respondents in low effect, while 36 in high. Extreme heat frequently causes this kind of psychological distress because discomfort, exhaustion, and sleep deprivation all work together to undermine mental stability during extreme heat exposure. Furthermore, feeling frustrated and powerless is exacerbated when heat stress prevents one from working or earning. On the contrary, Trauma and PTSD were experienced by 11 respondents with low effect analyzing in Figure 16. At the same time, 7 in high and social isolation (13 in low effect and 11 in high effect) was also noted, indicating that people tend to avoid social gatherings or outdoor contacts during periods of intense heat, which can result in loneliness and a decrease in social support. People who suffer from heat-related illnesses regularly may acquire a persistent fear or anxiety of being outside. Furthermore, people experienced economic hardship associated with psychological stress (4 in low effect and 13 in high), indicating the strong correlation between mental discomfort and livelihood uncertainty

3.10.1.3 Impacts on Pregnant Women's Health

It has been observed that heatwaves have a detrimental effect on the health of pregnant women. 35 in the high-effect group and 40 in the low-effect group experienced heat-related illness. During pregnancy, body temperature is elevated due to hormonal imbalance, which is why in this sensitive period, heatwaves become more severe for them. This explains why 9 in high effect and 14 in low effect faced complications during pregnancy and delivery, fetal development issues (13 people in low effect and 7 in high), and preterm labour (11 in low effect

and 7 in high effect) were also reported. These results show that pregnant women are among the most affected by heatwave exposure.

3.10.1.4 Community Health Impacts

At the community level, heatwave exposure had severe impacts, with health issues affecting 25 people in low effect and 17 people in high effect, and mental health challenges being commonly reported (22 in low effect and 19 in high effect). Heat exacerbates chronic conditions such as cardiovascular disease, diabetes, and respiratory illnesses by placing additional strain on the heart and lungs. Increased mortality has also been a great matter of concern here, as it was experienced by 19 people in low while 17in high effect, and healthcare strain (17 in both categories) was also significant. The health findings demonstrate that heatwaves have been a severe problem for people in the Khulna region, resulting in both physical and psychological issues. Heatwaves pose a significant threat to public health in tropical regions, exacerbated by poor living conditions, limited access to cooling, and high humidity.

3.10.2 Socio-Economic Impacts of Heatwaves

The Bivariate analysis also demonstrates that heatwaves have an acute impact on the socio-economic sector of the Khulna region.

3.10.2.1 Economic Effects on Personal Income

The most reported impacts were productivity loss (34 cases in low effect and 22 in high effect) and earnings loss (32 cases in low effect and 26 in high effect), with some individuals having to switch professions. These mostly occur because intense heat reduces the body's ability to perform tasks. To prevent heat exhaustion, workers, particularly those in outdoor industries such as construction, agriculture, and transportation, should slow down or take more frequent breaks. This immediately lowers their daily income. Furthermore, homelessness (2 in low effect, 0 in high effect) and unemployment (4 in both categories) were small but alarming, suggesting that prolonged financial strain during recurrent heat waves may lead to job instability and even displacement. Moreover, missing workdays due to heat illness directly impacts the security of livelihoods for those in the unorganized sector.

3.10.2.2 Agricultural Crop Impacts

The agricultural data showed in Fig. 18 that heatwaves have a detrimental effect on crops, where many respondents reported heat stress (34 in low effect and 25 in high effect) and water stress (29 in low effect and 18 in high effect). During hot weather, soil moisture quickly evaporates, reducing crop water availability and leading to wilting or reduced yields. Pollination decline was also reported by 10 as having a low effect and nine as having a high effect, and pest outbreaks (18 low, 14 high) were also noted. Warmer weather often promotes pest reproduction and reduces pollinator activity, particularly bee activity, thereby lowering the fertilization of flowering crops. Such agricultural disturbances have a detrimental effect on the food supply and income of smallholder farmers.

3.10.2.3 Impacts on Farmer Income and Agricultural Livelihood

The highest reported effect in this category was reduced yield, with 45 respondents (low) and 30 (high) marking it as a concern. Yield reduction directly translates to income loss, debt accumulation, and food insecurity. Increased production costs (18 low, 18 high) were also standard, as farmers must invest more in irrigation, fertilizers, and pest control to sustain crops in heat-stressed conditions. Rural impacts (10 low, nine high) and food chain disruption (7 low, nine high) further indicate that when yields fall, local food availability and prices fluctuate, affecting the entire rural economy. This demonstrates how heatwaves create a feedback cycle, reduced production leads to income instability, which limits the ability to invest in adaptive technologies.

3.10.2.4 Common Health Risks During a Heatwave

Some common health risks have been mentioned during the heatwave in Fig. 19, including heatstroke, which affected 27 people at low effect and 21 at high effect. Dehydration and heat exhaustion were also reported, with 25 experiencing low effect, 33 experiencing high effect, and 22 experiencing both low and high effect, respectively. Headache has been reported by 17 as low effect and 21 as high effect, with extreme heat exposure as the cause.

3.10.2.5 Direct Effect of Heatwave on Individuals

The direct effects of heatwaves on individuals have been reported as severe in Fig. 19. 35 respondents reported dehydration as having a low effect, and 30 as having a high effect, and a lack of purified water during this time was reported by 21 as having a low effect, and 27 as having a high effect, indicating that heatwaves intensify water insecurity and increase daily hardship. Additionally, prolonged exposure to high temperatures increases fluid loss, particularly among those without access to purified water, making heatwaves a severe problem for people. Moreover, poor hygiene and sanitation problems were experienced by 16 in low effect, and 5 in high effect, and waterborne diseases (16 in low effect and 5 in high effect) were also reported. Though poor hygiene was reported by 1 in low effect and 0 in high effect, this shows that limited water availability during the heatwave hampers sanitation efforts. Together, these circumstances strain household well-being and increase vulnerability in communities with limited resources.

3.10.2.6 Vulnerable Population Groups affected by Heatwave

The survey found elderly people to be the most vulnerable group during heatwaves in Fig. 19, with 31 reporting a low effect and 29 a high effect. Children (as experienced by 27 in the low-effect group and 19 in the high-effect group) were the second-most affected group, as their bodies are less able to adapt to temperature fluctuations. Outdoor workers also faced considerable exposure risk due to long working hours under direct sunlight, as experienced by 23 in low effect and 25 in high effect. Additionally, People suffering from long-term illness are also a vulnerable group, experiencing 20% in low effect and 18% in high effect, as they do not have the immunity to resist the heatwave-related illness. These findings highlight the uneven burden of heat impacts across social and occupational groups.

3.10.2.7 Effect of Heatwaves on Different Household Income Sources

The analysis of Fig. 20 also reveals that heatwaves caused some noticeable economic disruptions, particularly through reduced work capacity and lower returns from informal employment. 24 individuals in low effect experienced investment losses, and 7 in high effect, and decreased employment income was reported by 16 in low effect and 12 in high effect, indicating declining productivity under prolonged heat stress. Government benefits (6 low, 1 high) were rarely utilized, indicating a lack of social safety nets to alleviate financial strain. Many respondents also experienced decreased earnings from other sources of income, with 24 reporting a low effect and 21 a high effect.

3.10.2.8 Occupational Shifts Triggered by Heatwaves

Significant disruptions were found in heat-exposed sectors, according to occupational data. The most affected groups were construction workers (39 experienced low effect; 24 experienced high effect), outdoor service providers (26 experienced low effect; 23 experienced high effect), and agricultural labourers (18 experienced low effect; 18 experienced high effect). High temperatures immediately affected the security of one's livelihood by limiting outdoor working hours and impairing physical performance. Even industrial workers shifted their occupation due to rising workplace temperatures and safety concerns (9 low, five high). These findings demonstrate how labour patterns, economic stability, and personal health are affected by extreme heat, showed in Fig. 20.

3.10.2.9 Disruptions in Access to Essential Goods and Services

Water scarcity was noted by 32 respondents in both the low and high effect categories in Fig. 15, making it the most severe impact. This occurs because during heatwaves, reduced rainfall and high evaporation lower the available surface and groundwater levels. Healthcare disruption was also a noticeable issue, with 26 reporting low effects and 23 high effects. The frequent reports of food shortages (13 in low effect and 15 in high effect) and price rises (13 in low effect and 14 in high effect) indicate that extreme temperatures disrupt the food supply. Most likely, it happened because heat stress damages roads and spoils crops, lowering crop quality and productivity. The limited supply and rising costs of commodities in the marketplace exacerbate food insecurity among low-income individuals.

3.10.2.10 Livestock Health

The analysis also shows that heatwaves harm livestock health and rural livelihoods. Many responders reported animal deaths (38 in low effect and 29 in high effect) as a result of prolonged heat stress, dehydration, and reduced feed intake. The animals experience difficulties due to the extreme temperatures, which affect their ability to regulate body temperature, causing physiological strain, impairing immunity, and increasing the risk of illness. Reduced milk production (13% in low effect and 20% in high effect) and reduced feed intake (30% in low effect and 23% in high effect) were also significant issues in the Khulna region in Fig. 15. Degraded pasture limits nutrient delivery, while high temperatures reduce appetite and feed conversion efficiency. During the heatwave, the quantity and quality of milk produced by dairy animals are reduced due to hormonal imbalance and metabolic instability. A smaller group reported inferior meat quality, which was associated with a low effect (1) and

a high effect (7), and an altered metabolic rate was reported by 10 with a low effect and 5 with a high effect, all of which were indicators of persistent physiological stress.

3.10.2.11 Electricity and Distribution

During heatwaves, the energy sector faces significant strain. The analysis shows in Fig. 18 a considerable rise in electricity usage, with 36 experiencing low effect and 37 experiencing high effect, as houses and businesses increasingly depend on cooling systems. This demand often exceeds grid capacity due to power unit overheating and a lack of water for cooling thermal plants, which reduces generation efficiency, resulting in 23% in low effect and 13% in high effect. It was also noted that distribution issues (20 in low, 19 in high) and higher economic costs (22 in low, 17 in high) were reported by the responders. Frequent power outages affect businesses, industries, and public services, including hospitals and water treatment facilities. When electrical systems overheat and malfunction, maintenance costs rise because infrastructure resilience and environmental stress are interconnected.

3.11 Regression Analysis of Health and Economy Impacts

The table 5 & 6 illustrate the various ways in which heat waves impact the health and economy of the Khulna City area. There is a 1.29 times greater chance that facing problems with water will have a health effect, with a range of 0.72 to 2.32. However, the p-value is greater than 0.05, indicating that this link is not statistically significant. Households with older people are much more likely to have health problems during heat waves, with an odds ratio of 6.73 ($p < 0.001$). Homes with outdoor workers have an even higher odds ratio of 11.83 ($p < 0.001$), indicating a strong association between outdoor work and health risks during heat waves. Families with chronically ill members also had a statistically significantly higher risk of health problems, with an odds ratio of 3.54 ($p < 0.05$). This illustrates how vulnerable these individuals are when the temperature rises. Dehydration is another serious health issue, with a 7.76 odds ratio ($p < 0.001$), indicating the severity of this problem during heat waves. There is also a strong link between the inability to obtain clean water and health problems, with an odds ratio of 19.4 ($p < 0.001$). This research highlights the importance of clean water in mitigating the health impacts of heatwaves. There is a 1.98% chance that poor hygiene and sanitation would cause health problems during heat waves, but this number is not statistically significant. The dataset shows an odds ratio of 29.35 ($p < 0.001$) for death rates, which means that death rates go up a lot when it's hot. There is also an odds ratio of 12.79 ($p = 0.01$), indicating a significant decrease in meat quality during these periods. These changes could make it more difficult for people in the area to access food.

4 Conclusion

This study seeks to examine the spatiotemporal variation of temperature and land use in Khulna City Corporation (KCC) using Land Use and Land Cover (LULC), Land Surface Temperature (LST), Normalized Difference Vegetation Index (NDVI), and Normalized Difference Built-up Index (NDBI) to understand their combined impact on Urban Heat Island (UHI) intensity. Bangladesh is extremely vulnerable to climate-induced hazards like heatwaves (HWs), but there is a paucity of studies on the urban heat risk of Khulna despite rapid urbanisation and

increased thermal stress. Using ArcGIS, Principal Component Analysis (PCA), and household survey data, the study provides an in-depth assessment of the urban heat phenomenon and its effects on human health and economic productivity. The results show a significant transformation of the urban landscape from 1995 to 2025, from a vegetation cover of 72.21% to 45.09% and a built-up area of 10.12% to 32.16%, which is a rapid urbanization process. The thermal conditions deteriorated, where the Land Surface Temperature (LST) in the area above 40°C increased from 44% in 2015 to 67% in 2025. The correlation analysis shows an almost perfect positive correlation between LST and urban heat island (UHI) intensity ($r \approx 0.99$) and a negative correlation between the Normalized Difference Vegetation Index (NDVI) and LST, confirming the cooling effect of vegetation. Principal Component Analysis (PCA) further identified LST, Normalized Difference Built-up Index (NDBI), and Land Use Land Cover (LULC) as the major factors influencing urban thermal variability and heatwave trends. The survey indicated a significant socio-economic vulnerability to the impacts of exposure to heatwaves. Sleep disruption (36.7%) and heat-related discomfort (35.6%) were the most commonly reported impacts, while high stress (23.2%) was less common. Pregnant women (55.2%) were the most vulnerable group, followed by the elderly (31.6%) and outdoor workers (27.5%), whereas children (22%) were less affected. Heat exposure was also associated with adverse pregnancy outcomes, especially preterm labour (16.1%) and developmental risks (14.3%). From an economic point of view, heatwaves caused reduced labour productivity, occupational changes, and losses in agriculture, livestock, and essential services. The major stressors that affected household wellbeing and economic stability were water scarcity (40%), increased food prices (23.8%), and power outages. The results indicate that heatwaves are not only environmental hazards but also important socio-economic and development challenges. Integrating heatwave risk reduction in urban planning, economic development plans, and climate adaptation policies can help reduce future vulnerabilities and foster sustainable urban development. Addressing these issues requires climate-sensitive planning, improvement of green infrastructure, LST mapping, heatwave vulnerability assessments, and enhanced public awareness among the vulnerable population. The study is limited by the use of 30 m spatial resolution satellite data, which may not capture fine-scale thermal variations, and by limited ground observations for validation. Future studies should include higher resolution thermal data, in-situ measurements, and detailed socioeconomic and health data to improve urban heat assessments. The study provides useful evidence for policymakers, planners, and researchers for formulating effective heat adaptation measures and promoting climate-resilient urban development in Bangladesh.

Declaration of Competing Interest: The authors declare that they have no known competing financial interests or personal relationships that could have appeared to influence the work reported in this paper.

Funding Statement: This research received no specific grant from any funding agency in the public, commercial, or not-for-profit sectors.

Author Contribution Statement:

Halima Akter, Dipok Chandra Nath, Md. Abdur Rahman Bijoy: Conceptualization, Formal analysis, Investigation, Methodology, Resources, Software, Validation, Visualization, Writing – original draft, Writing – review & editing

Md. Riajul Islam, Hasan Shariar Shawron, Musrat Mehjabin Asha, Muhammad Iftekhar Uddin, Esrat Jahan Papri: Formal analysis, Investigation, Methodology, Resources, Software, Validation, Visualization, Writing – original draft, Writing – review & editing.

Md Shafiqul Islam: Visualization, Writing – original draft, Writing – review & editing.

Irteja Hasan: Conceptualization, Investigation, Methodology, Resources, Software, Supervision, Visualization, Writing – original draft, Writing – review & editing

References

Mannan, M. A., Akter, F., Rashid, M. B., Hossain, M. M., Faruque, S. O., Ara, S. S., ... & Chowdhury, M. A. M. (2022). An analytical study of Heat Wave occurred over Bangladesh during pre-monsoon of 2021. Dew-Drop, 8, 152-160.

Adnan, M. S. G., Kabir, I., Hossain, M. A., Chakma, S., Tasneem, S. N., Saha, C. R., Hassan, Q. K., & Dewan, A. (2024). Heatwave vulnerability of large metropolitans in Bangladesh: An evaluation. *Geomatica*, *76*(2). https://doi.org/10.1016/j.geomat.2024.100020

Dong, W., Liu, Z., Zhang, L., Tang, Q., Liao, H., & Li, X. (2014). Assessing heat health risk for sustainability in Beijing's urban heat island. *Sustainability (Switzerland)*, *6*(10), 7334–7357. https://doi.org/10.3390/su6107334

Hossain, I., Rana, M. S., Haque, A. K. M. M., & Al Masud, A. (2024). Urban Household Adaptation to Extreme Heatwaves: Health Impacts, Socioeconomic Disparities, and Sustainable Strategies in Rajshahi. *Discover Sustainability*, *5*(1). https://doi.org/10.1007/s43621-024-00697-2

Huang, H., Deng, X., Yang, H., Li, S., & Li, M. (2020). Spatial evolution of the effects of urban heat island on residents' health. *Tehnicki Vjesnik*, *27*(5), 1427–1435. https://doi.org/10.17559/TV-20200503211912

Mirzaei, M., Verrelst, J., Arbabi, M., Shaklabadi, Z., & Lotfizadeh, M. (2020). Urban heat island monitoring and impacts on citizen's general health status in Isfahan metropolis: A remote sensing and field survey approach. *Remote Sensing*, *12*(8). https://doi.org/10.3390/RS12081350

Nadeem, F., Tariq, S., Haq, Z. U., & Khan, H. S. (2022). *Investigating the synergies between the Urban Heat Island (UHI) and Heatwaves (HWs)*. https://doi.org/10.21203/rs.3.rs-2080699/v1

Nissan, H., Burkart, K., de Perez, E. C., Van Aalst, M., & Mason, S. (2017). Defining and predicting heat waves in Bangladesh. *Journal of Applied Meteorology and Climatology*, *56*(10), 2653–2670. https://doi.org/10.1175/JAMC-D-17-0035.1

Nureen, N., Hafiz, S. B., & Nureen, N. (2024). *Integrated Assessment of Heatwave Vulnerability in Khulna City: A Multi-Factor Index*. https://icace2024.cuet.ac.bd

Rahman, M. N., Rony, M. R. H., Jannat, F. A., Pal, S. C., Islam, M. S., Alam, E., & Islam, A. R. M. T. (2022). Impact of Urbanization on Urban Heat Island Intensity in Major Districts of Bangladesh Using Remote Sensing and Geo-Spatial Tools. *Climate*, *10*(1). https://doi.org/10.3390/cli10010003

Agresti, A. (2018). *Statistical methods for the social sciences*. Pearson.

Altman, D. G. & Royston, P. (2006). The cost of dichotomising continuous variables. In *British Medical Journal* (Vol. 332, Issue 7549, p. 1080). https://doi.org/10.1136/bmj.332.7549.1080

Ananth, C. V & Kleinbaum, D. G. (1997). Regression Models for Ordinal Responses: A Review of Methods and Applications and Kleinbaum D G. Regression models for ordinal responses: A review of methods and applications. In *International Journal of Epidemiology © International Epidemiological Association* (Vol. 26, Issue 6).

Bland, J. M. & Altman, D. G. (2000). The odds ratio. *BMJ*, *320*(7247), 1468. https://doi.org/10.1136/bmj.320.7247.1468

Fayers, P. M. & Hand, D. J. (n.d.). *Causal variables, indicator variables and measurement scales: an example from quality of life*. https://academic.oup.com/jrsssa/article/165/2/233/7084159

García-León, D., Casanueva, A., Standardi, G., Burgstall, A., Flouris, A. D. & Nybo, L. (2021). Current and projected regional economic impacts of heatwaves in Europe. *Nature Communications*, *12*(1). https://doi.org/10.1038/s41467-021-26050-z

Hosmer, D. W., Lemeshow, S. & Sturdivant, R. X. (2013). *Applied logistic regression*. Wiley.

Menard, S. (2002). *Applied Logistic Regression Analysis* (2nd ed.). Sage Publications.

Niu, Y., Li, Z., Gao, Y., Liu, X., Xu, L., Vardoulakis, S., Yue, Y., Wang, J. & Liu, Q. (n.d.). *A Systematic Review of the Development and Validation of the Heat Vulnerability Index: Major Factors, Methods, and Spatial Units*. https://doi.org/10.1007/s40641-021-00173-3/Published

Rathi, S. K., Chakraborty, S., Mishra, S. K., Dutta, A. & Nanda, L. (2022). A heat vulnerability index: Spatial patterns of exposure, sensitivity and adaptive capacity for urbanites of four cities of india. *International Journal of Environmental Research and Public Health*, *19*(1). https://doi.org/10.3390/ijerph19010283.

Santamouris, M. (2020). Recent progress on urban overheating and heat island research. Integrated assessment of the energy, environmental, vulnerability and health impact. Synergies with the global climate change. In *Energy and Buildings* (Vol. 207). Elsevier Ltd. https://doi.org/10.1016/j.enbuild.2019.109482

Sestito, B., Reimann, L., Mazzoleni, M., Botzen, W. J. W., & Aerts, J. C. J. H. (2025). Identifying vulnerability factors associated with heatwave mortality: a spatial statistical analysis across Europe. *Environmental Research Letters* , *20*(4). https://doi.org/10.1088/1748-9326/adbcc8

Tan, J., Zheng, Y., Tang, X., Guo, C., Li, L., Song, G., Zhen, X., Yuan, D., Kalkstein, A. J., Li, F., & Chen, H. (2010). The urban heat island and its impact on heat waves and human health in Shanghai. *International Journal of Biometeorology*, *54*(1), 75–84. https://doi.org/10.1007/s00484-009-0256-x

Tran, D. N., Doan, V. Q., Nguyen, V. T., Khan, A., Thai, P. K., Cunrui, H., Chu, C., Schak, E., & Phung, D. (2020). Spatial patterns of health vulnerability to heatwaves in Vietnam.

International Journal of Biometeorology, *64*(5), 863–872. https://doi.org/10.1007/s00484-020-01876-2

Van Der Hoeven, F., & Wandl, A. (2015). Amsterwarm: Mapping the landuse, health and energy-efficiency implications of the Amsterdam urban heat island. *Building Services Engineering Research and Technology*, *36*(1), 67–88. https://doi.org/10.1177/0143624414541451

Vargo, J., Stone, B., Habeeb, D., Liu, P., & Russell, A. (2016). The social and spatial distribution of temperature-related health impacts from urban heat island reduction policies. *Environmental Science and Policy*, *66*, 366–374. https://doi.org/10.1016/j.envsci.2016.08.012

Xu, C., Wei, R., & Tong, H. (2025). A Systematic Review of Methodological Advances in Urban Heatwave Risk Assessment: Integrating Multi-Source Data and Hybrid Weighting Methods. In *Sustainability (Switzerland)* (Vol. 17, Issue 8). Multidisciplinary Digital Publishing Institute (MDPI). https://doi.org/10.3390/su17083747

Al Kafy, A., Al-Faisal, A., Mahmudul Hasan, M., Sikdar, M. S., Hasan Khan, M. H., Rahman, M., & Islam, R. (2020). Impact of LULC Changes on LST in Rajshahi District of Bangladesh: A Remote Sensing Approach. *Journal of Geographical Studies*, *3*(1), 11–23. https://doi.org/10.21523/gcj5.19030102

Avdan, U., & Jovanovska, G. (2016). Algorithm for automated mapping of land surface temperature using LANDSAT 8 satellite data. *Journal of Sensors*, *2016*. https://doi.org/10.1155/2016/1480307

Fatemi, M., & Narangifard, M. (2019). Monitoring LULC changes and its impact on the LST and NDVI in District 1 of Shiraz City. *Arabian Journal of Geosciences*, *12*(4), 127. https://doi.org/10.1007/s12517-019-4259-6

Gutman, G., Huang, C., Chander, G., Noojipady, P., & Masek, J. G. (2013). Assessment of the NASA–USGS Global Land Survey (GLS) datasets. *Remote Sensing of Environment*, *134*, 249–265. https://doi.org/https://doi.org/10.1016/j.rse.2013.02.026

He, B.-J., Zhao, Z.-Q., Shen, L.-D., Wang, H.-B., & Li, L.-G. (2019). An approach to examining performances of cool/hot sources in mitigating/enhancing land surface temperature under different temperature backgrounds based on landsat 8 image. *Sustainable Cities and Society*, *44*, 416–427. https://doi.org/https://doi.org/10.1016/j.scs.2018.10.049

Hu, Y., Hou, M., Jia, G., Zhao, C., Zhen, X., & Xu, Y. (2019). Comparison of surface and canopy urban heat islands within megacities of eastern China. *ISPRS Journal of Photogrammetry and Remote Sensing*, *156*, 160–168. https://doi.org/https://doi.org/10.1016/j.isprsjprs.2019.08.012

Matsushita, B., Yang, W., Chen, J., Onda, Y., & Qiu, G. (2007). Sensitivity of the Enhanced Vegetation Index (EVI) and Normalized Difference Vegetation Index (NDVI) to topographic effects: A case study in high-density cypress forest. *Sensors*, *7*(11), 2636–2651. https://doi.org/10.3390/s7112636

Muhamad, S. N., How, V., Lim, F. L., Akim, A., Karuppiah, K., Shabrina, N., & Mohd, A. (2024). Assessment of heat stress contributing factors in the indoor environment among vulnerable populations in Klang Valley using principal component analysis (PCA). *Scientific Reports*, 1–10. https://doi.org/10.1038/s41598-024-67110-w

Rahman, M. N., Rony, M. R. H., Jannat, F. A., Pal, S. C., Islam, M. S., Alam, E., & Islam, A. R. M. T. (2022). Impact of Urbanization on Urban Heat Island Intensity in Major Districts of Bangladesh Using Remote Sensing and Geo-Spatial Tools. *Climate*, *10*(1). https://doi.org/10.3390/cli10010003

947 Singh, A. (1989). Review Article Digital change detection techniques using remotely-sensed
948 data. *International Journal of Remote Sensing*, *10*(6), 989–1003.
949 https://doi.org/10.1080/01431168908903939
950

Figures

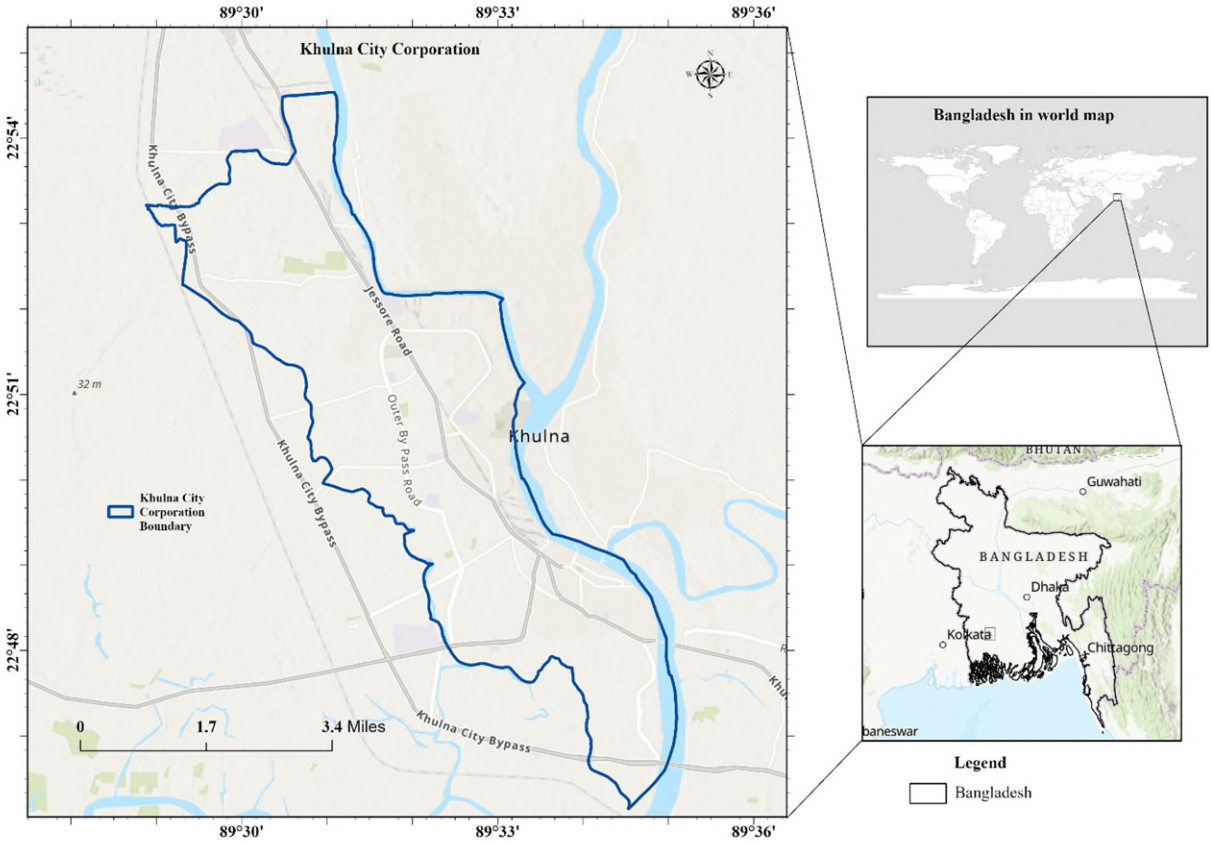


Fig 1: Study area location map and survey locations

Figures

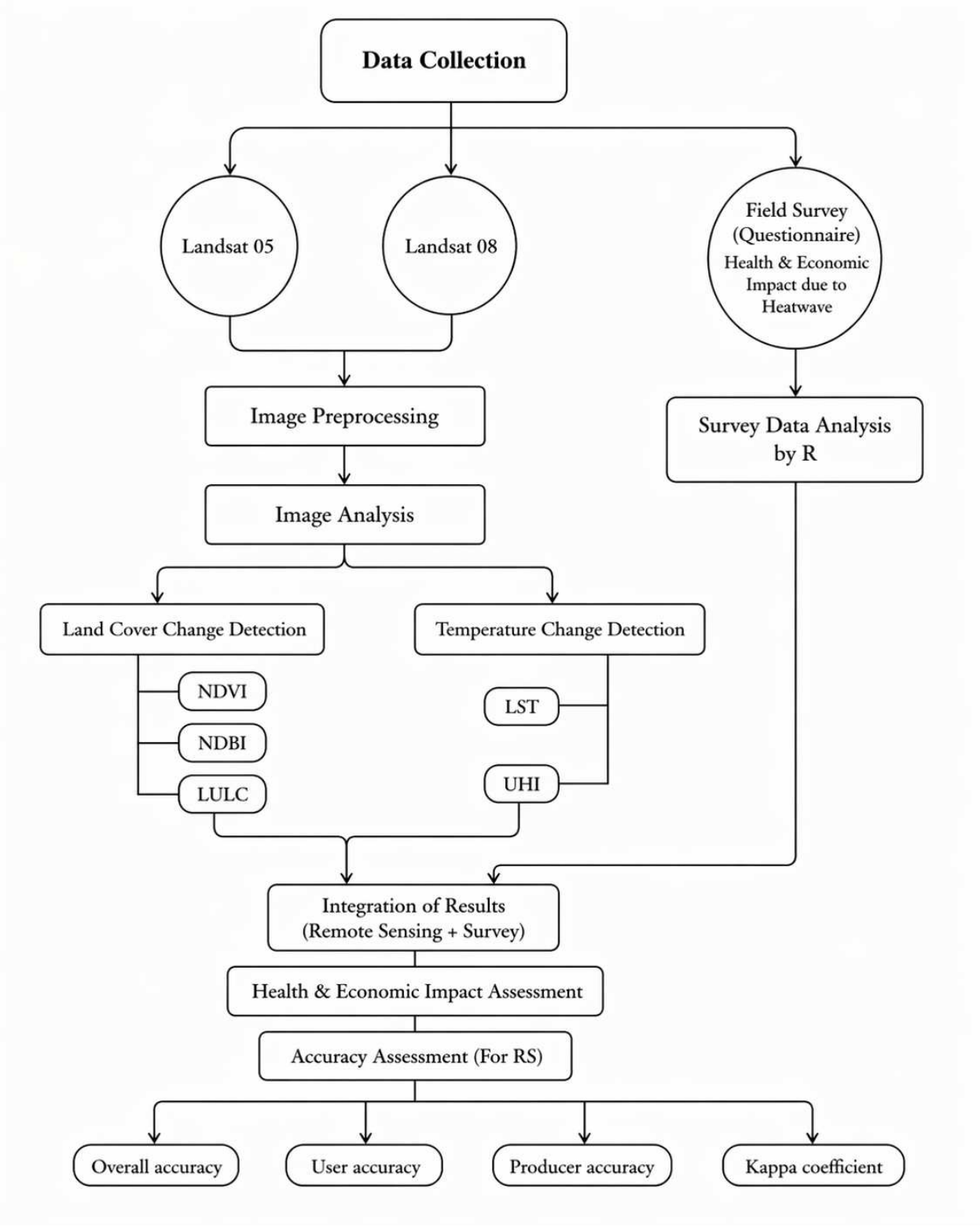


Fig 2: Methodology Flowchart

Figures

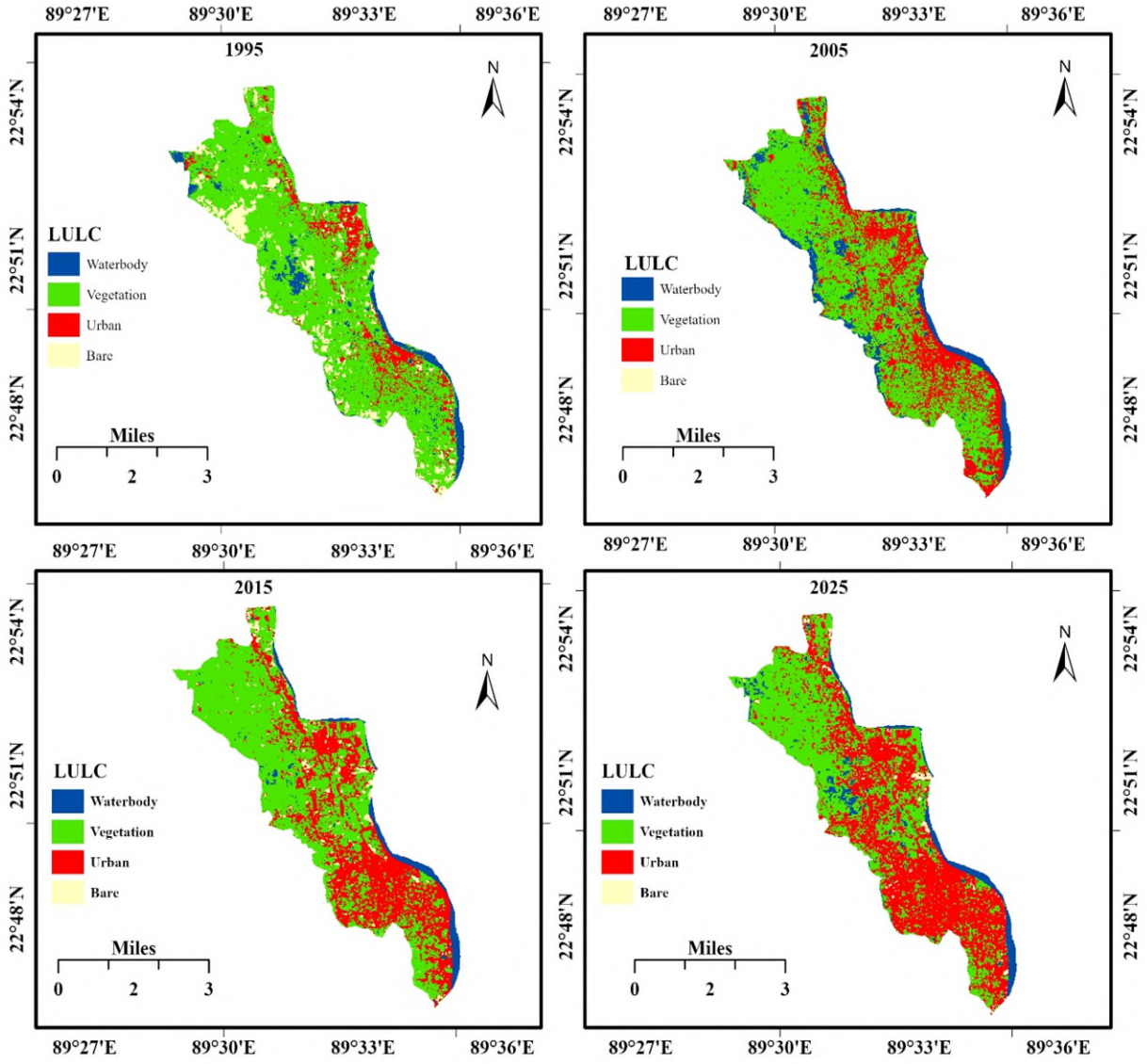


Fig. 3: Land use and land cover changes Map

Figures

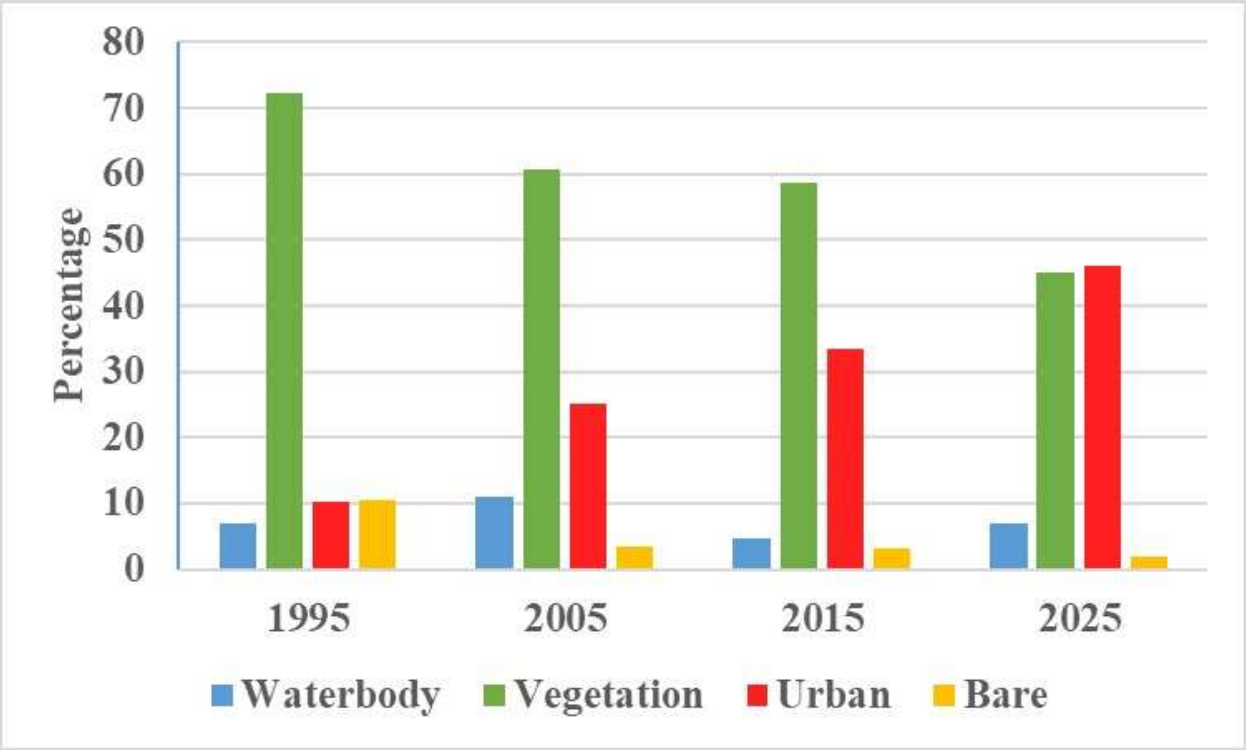


Fig. 4: Land use and land cover changes analysis

Figures

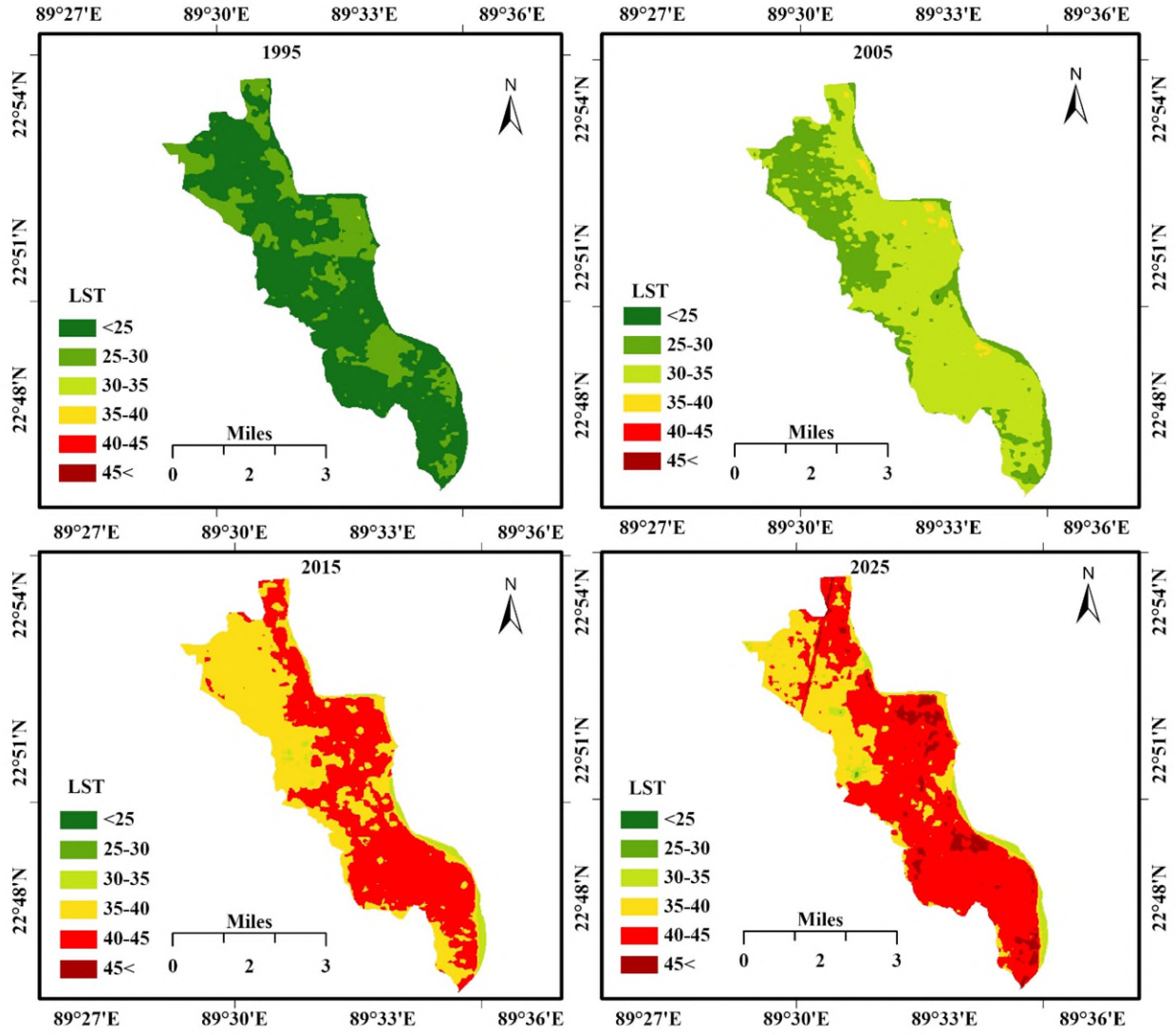


Fig. 5: Land surface temperature (LST) Analysis

Figures

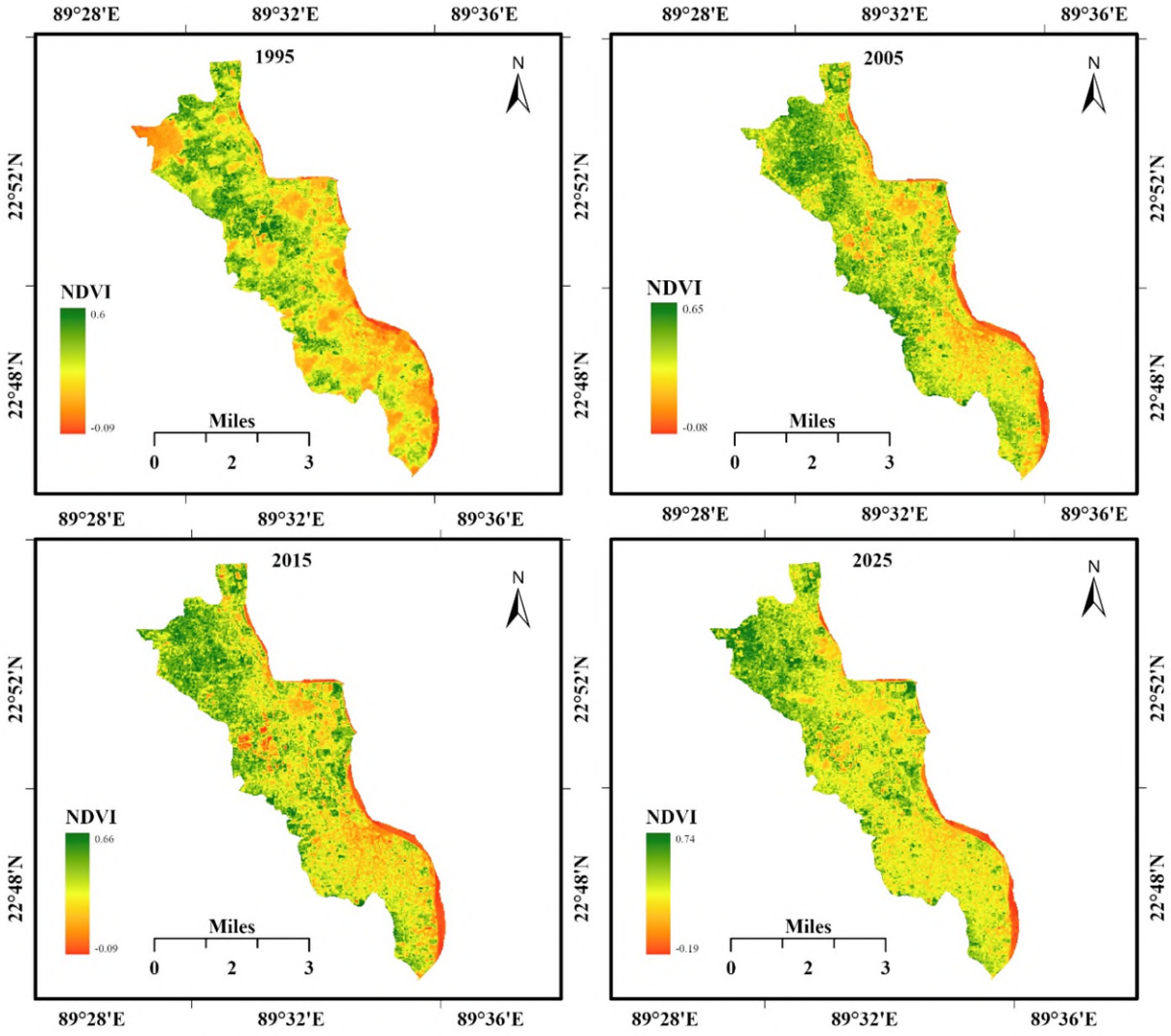


Fig. 6: Normalized Difference Vegetation Index (NDVI) Analysis

Figures

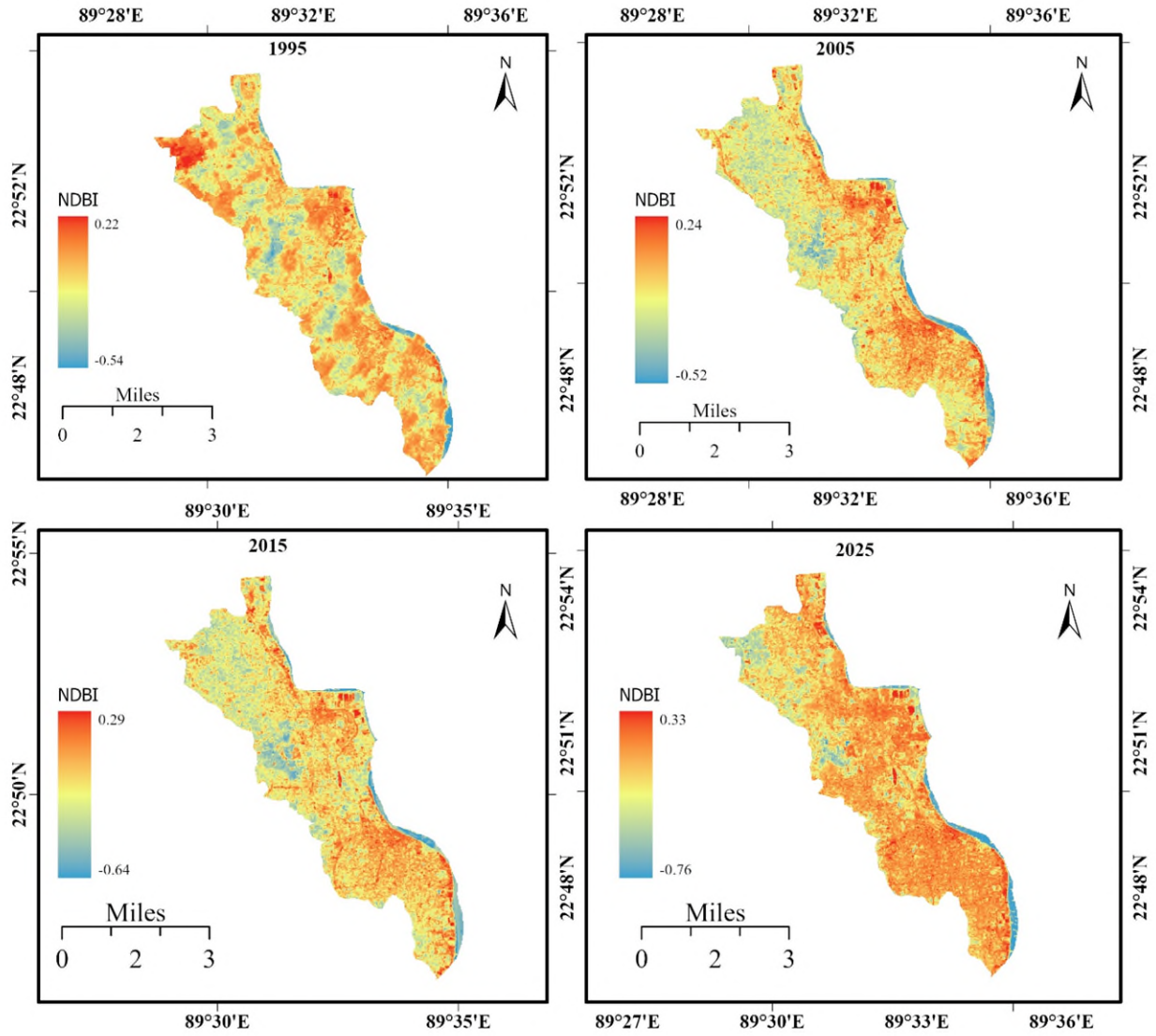


Fig. 7: Normalized Difference Built-up Index Analysis

Figures

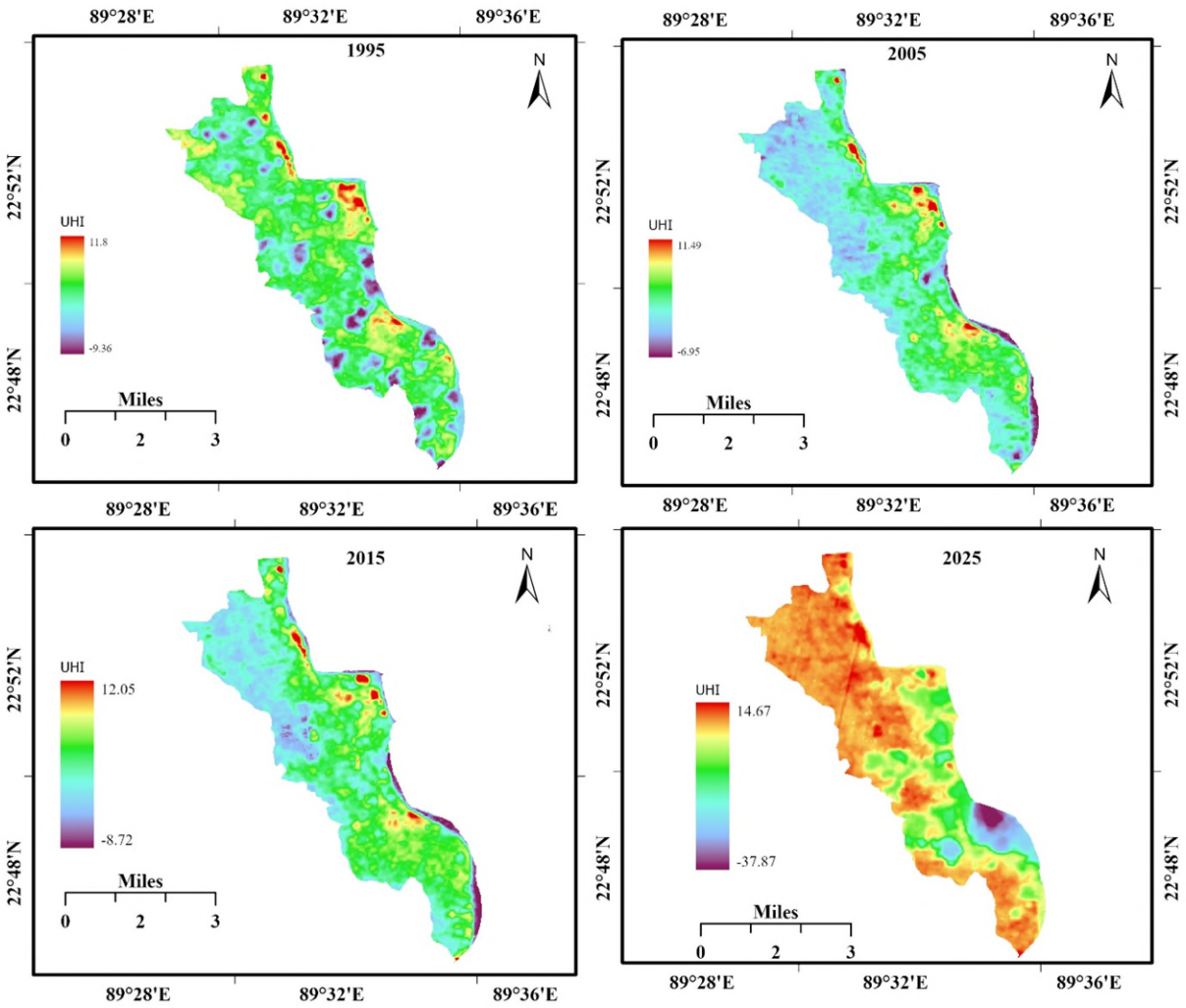


Fig. 8: Spatiotemporal dynamics of Urban Heat Island (UHI) intensity

Figures

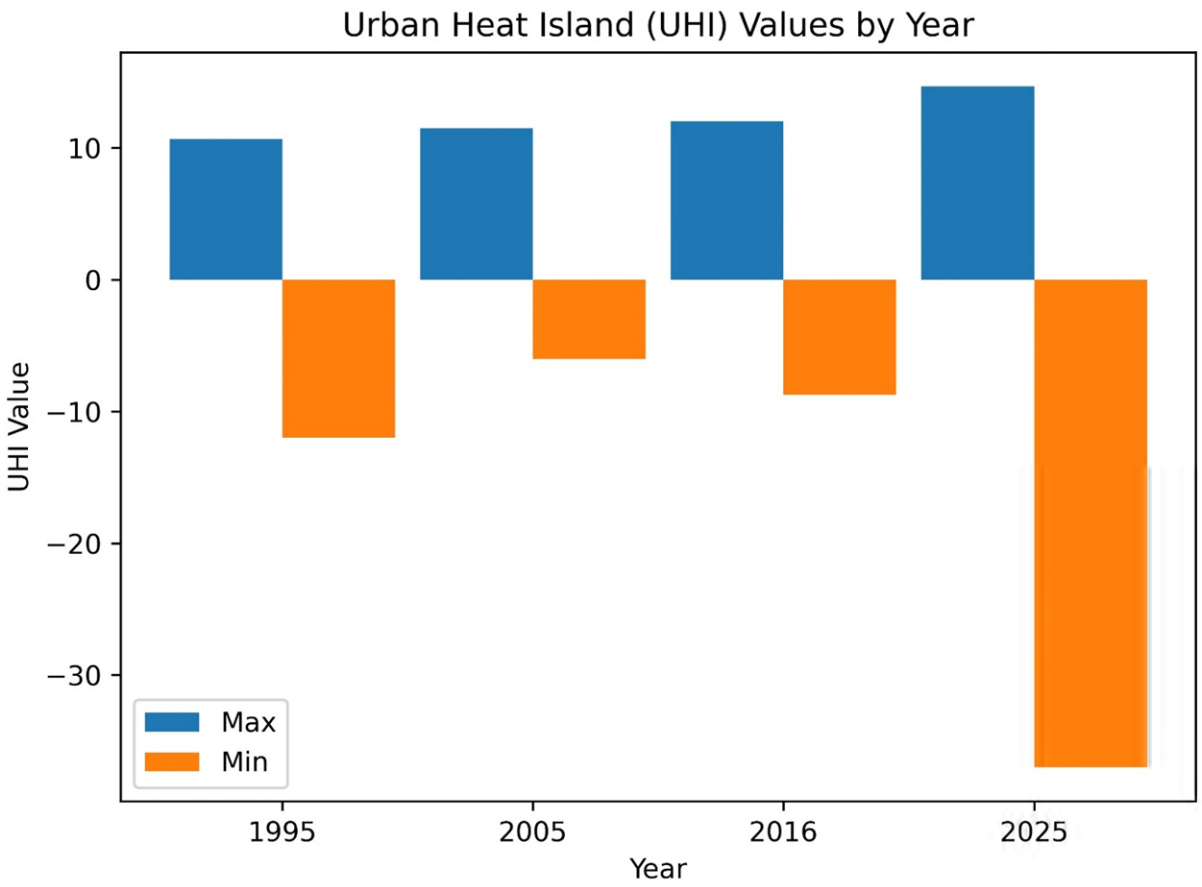
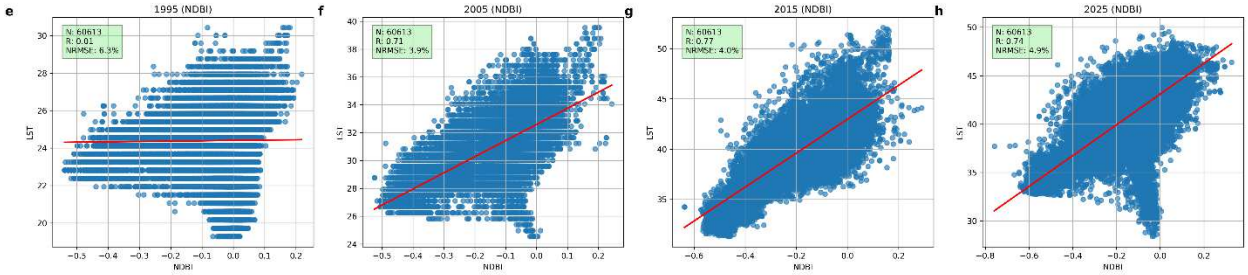
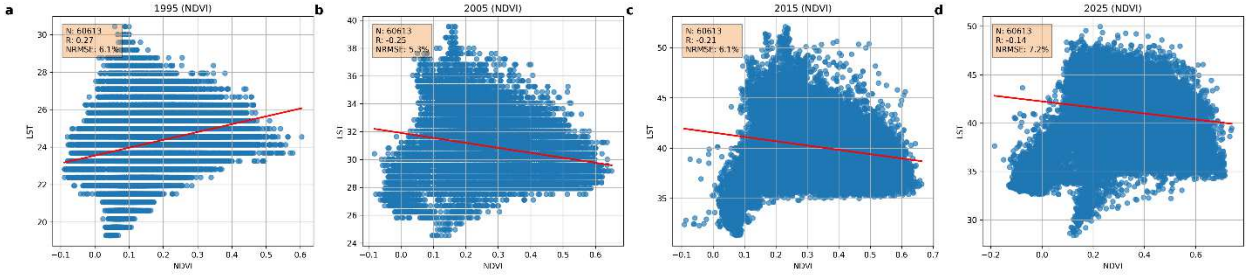


Fig. 9: Temporal variation of Urban Heat Island (UHI) statistics

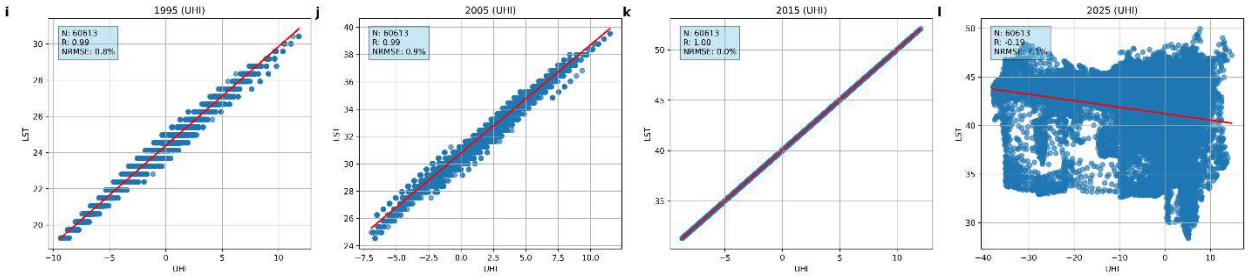
Figures



(a)



(b)



(c)

Fig. 10: Correlation between Land Use Indicators: (a) NDBI LST Correlation, (b) NDVI LST Correlation, (c) UHI LST Correlation

Figures

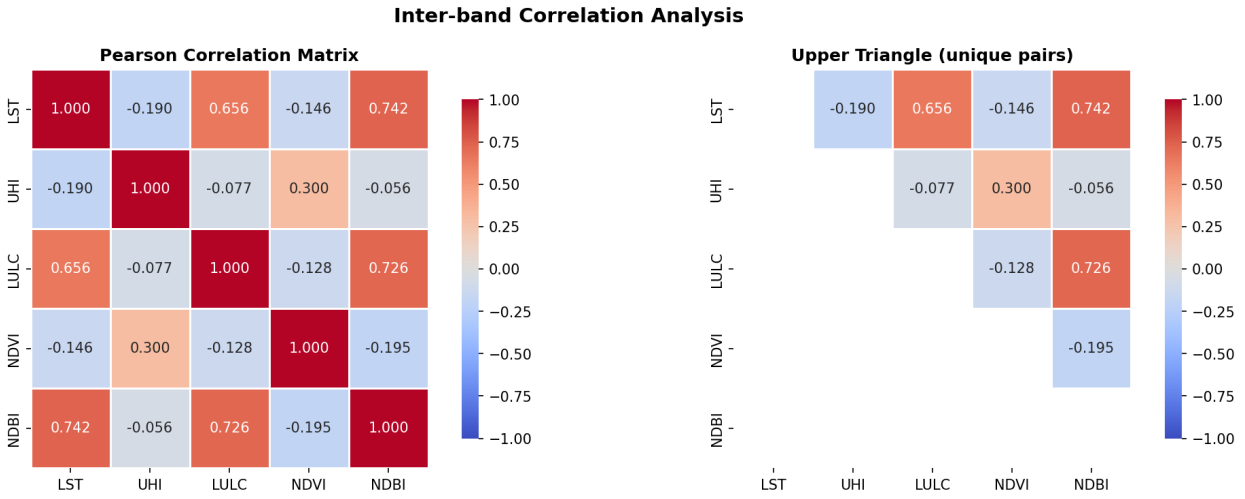


Figure 11: Inter-band Correlation Analysis of PCA

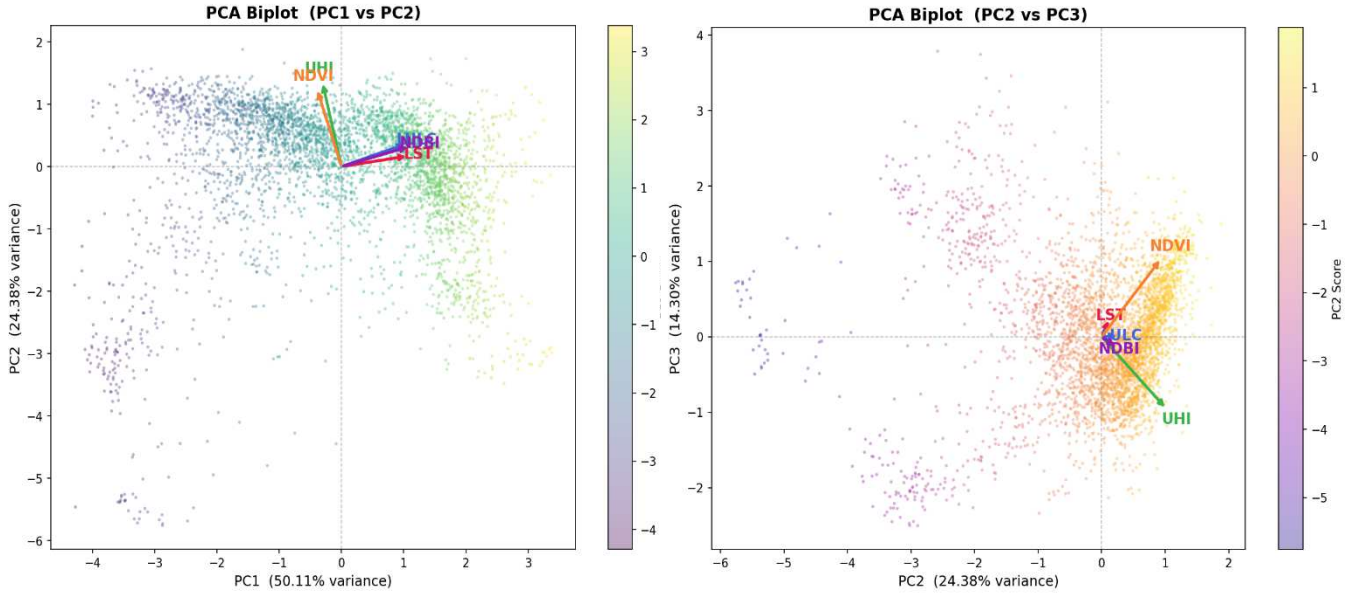


Figure 12: Principal Component Analysis (PCA) Biplots Showing Relationships Among UHI, NDVI, LST, and NDBI (PC1–PC2 and PC2–PC3)

Figures

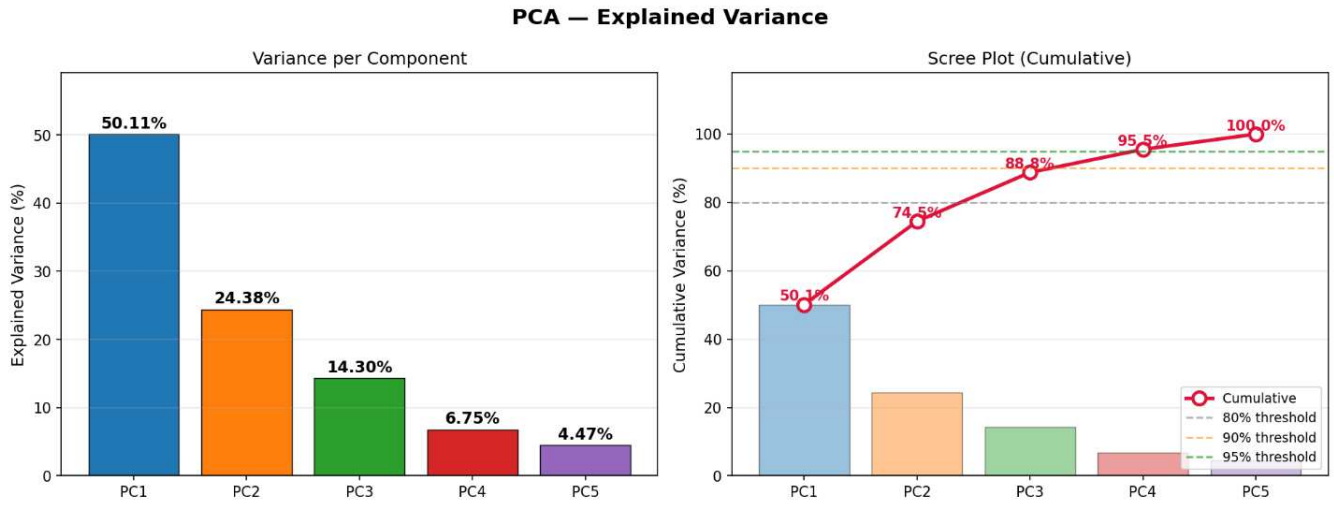


Figure 13: Explained Variance and Cumulative Variance of Principal Components Obtained from PCA.

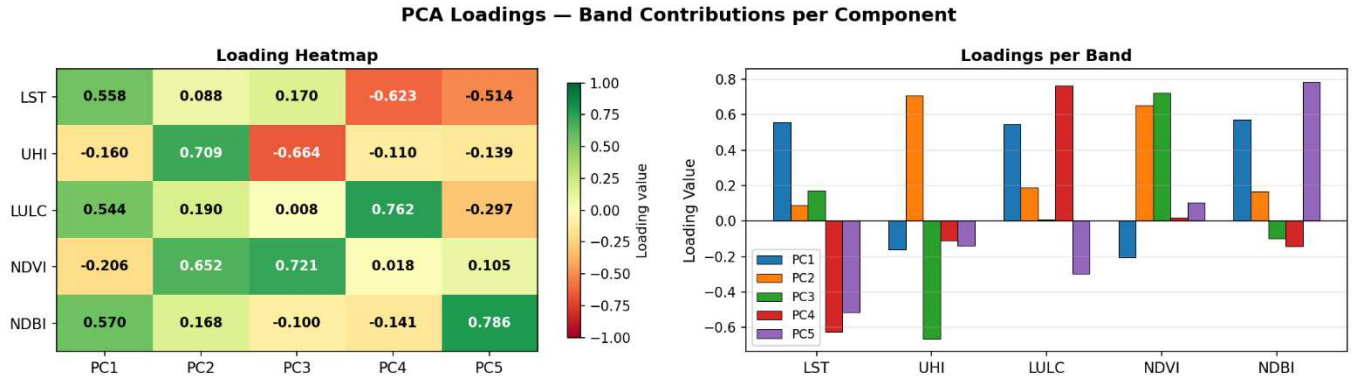


Figure 14: PCA Loadings- Band Contributions per Component

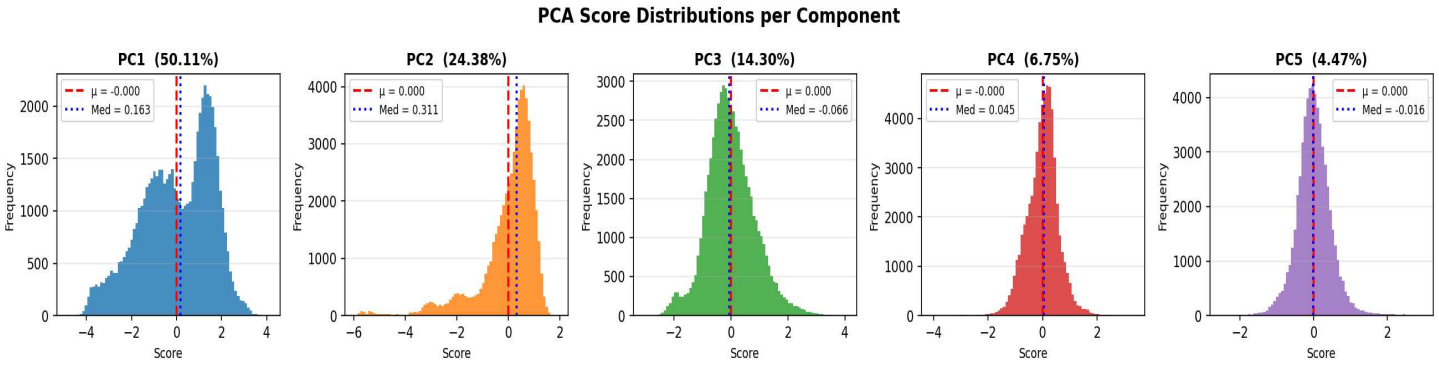


Figure 15: PCA Score Distributions per Component

Figures

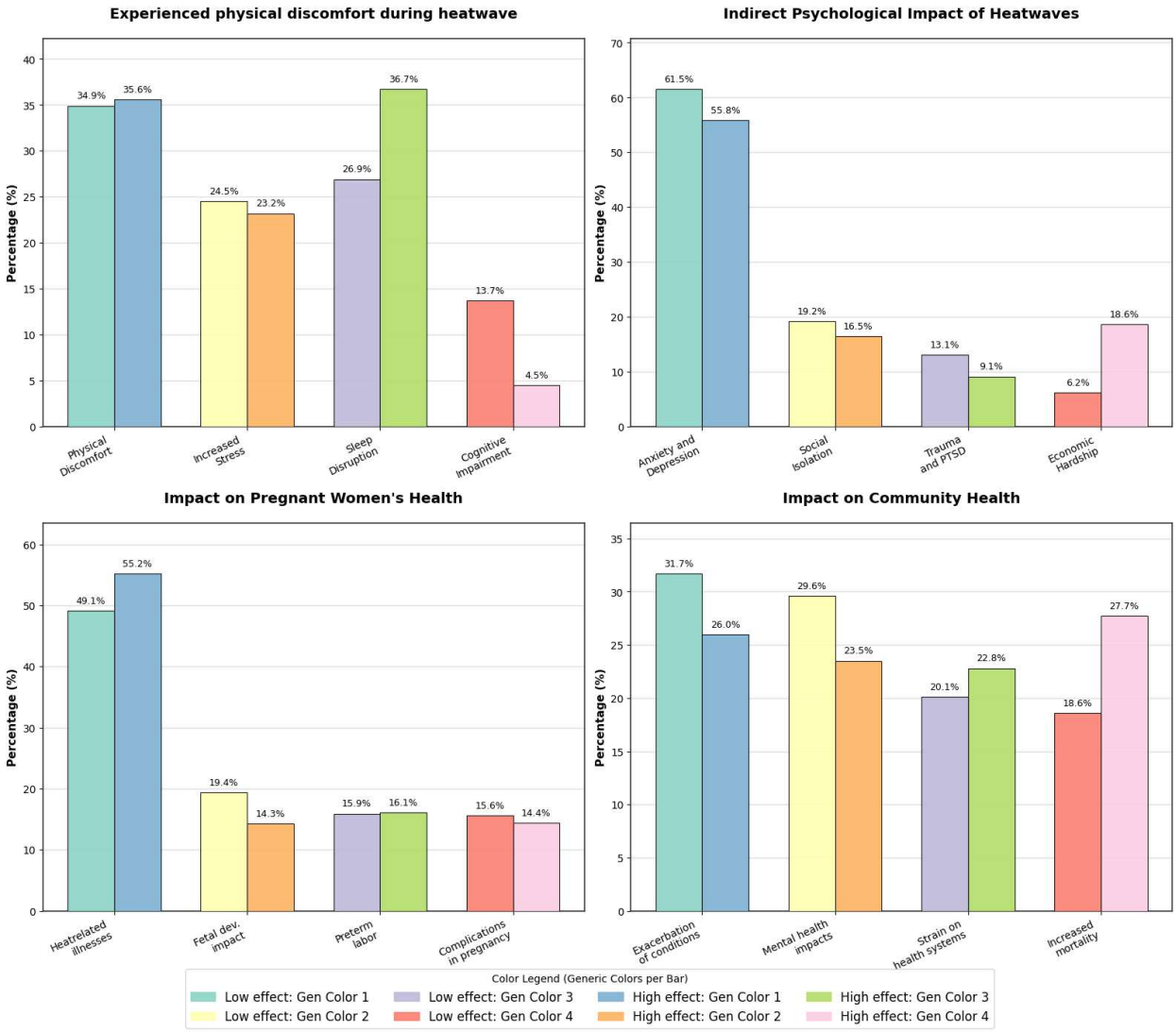


Fig. 16: Heatwave Impacts on Pregnant Women's Health

Figures

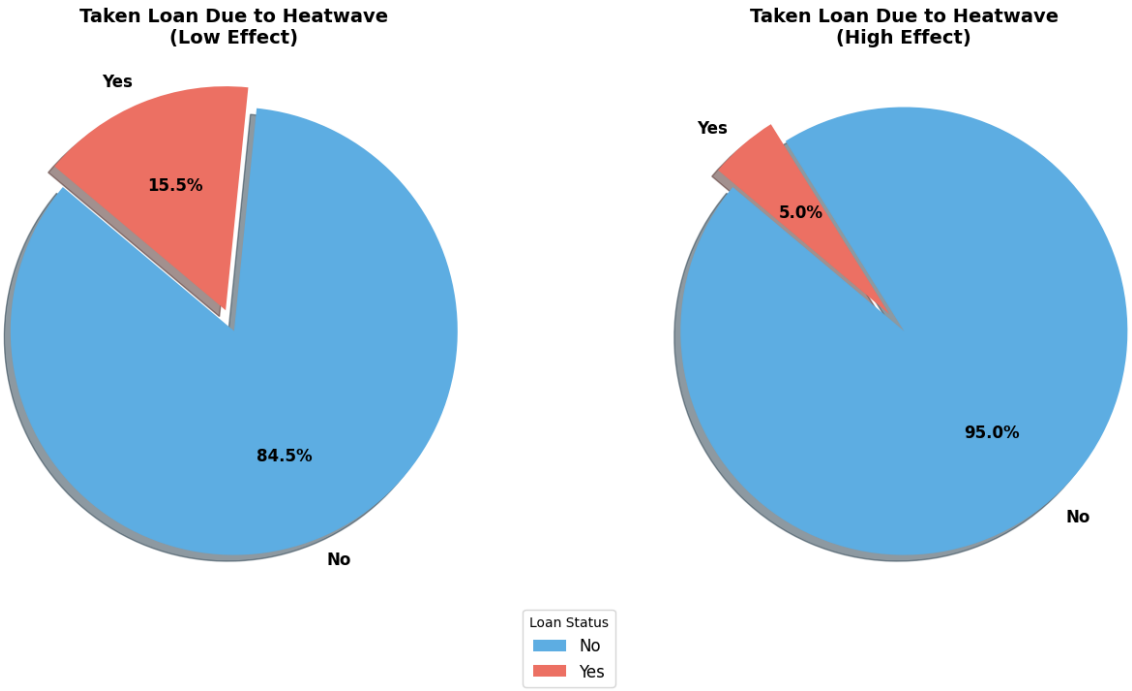


Fig. 17: Loan history due to the heatwave

Figures

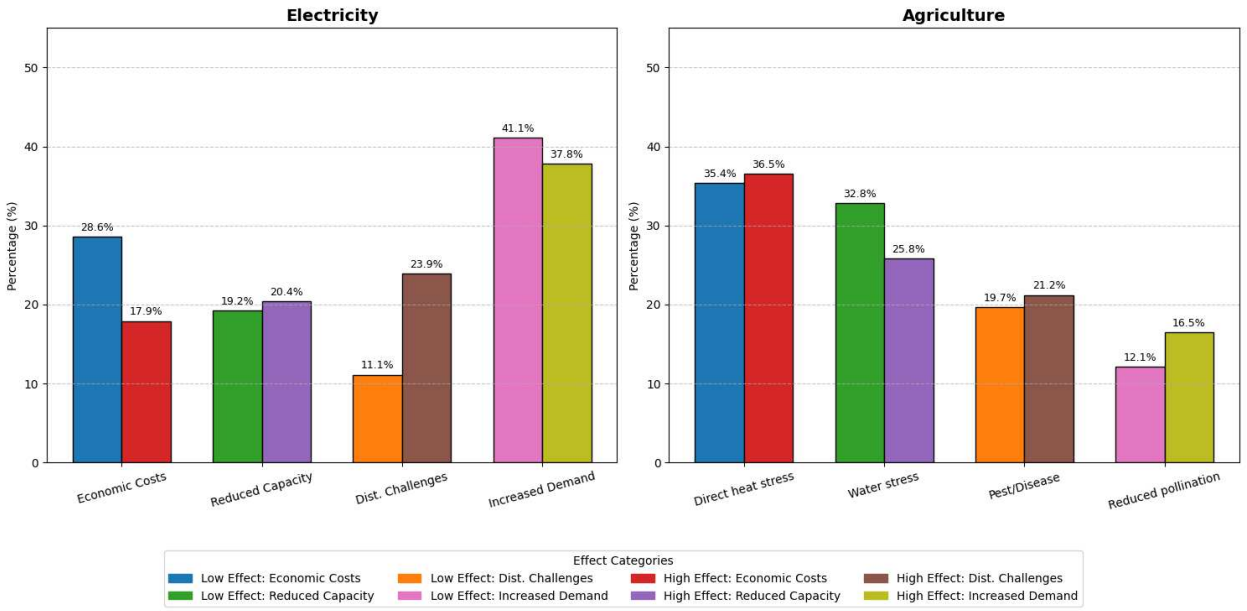


Figure 18: Electricity & Agricultural Crop Impacts due to heatwave

Figures

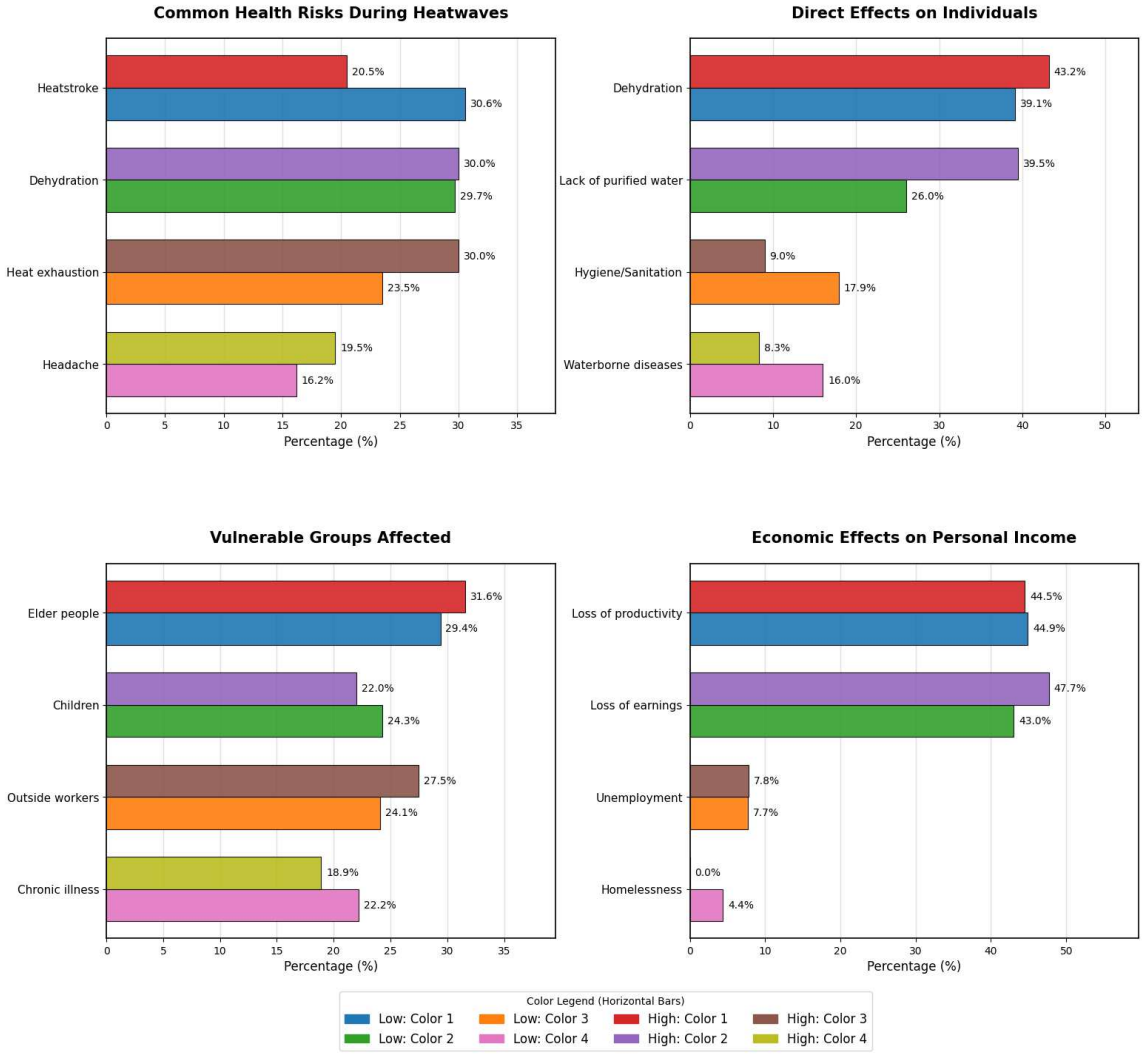


Fig. 19: Perceived Health Risks, Vulnerabilities, and Economic Impacts of Heatwaves in Khulna City

Figures

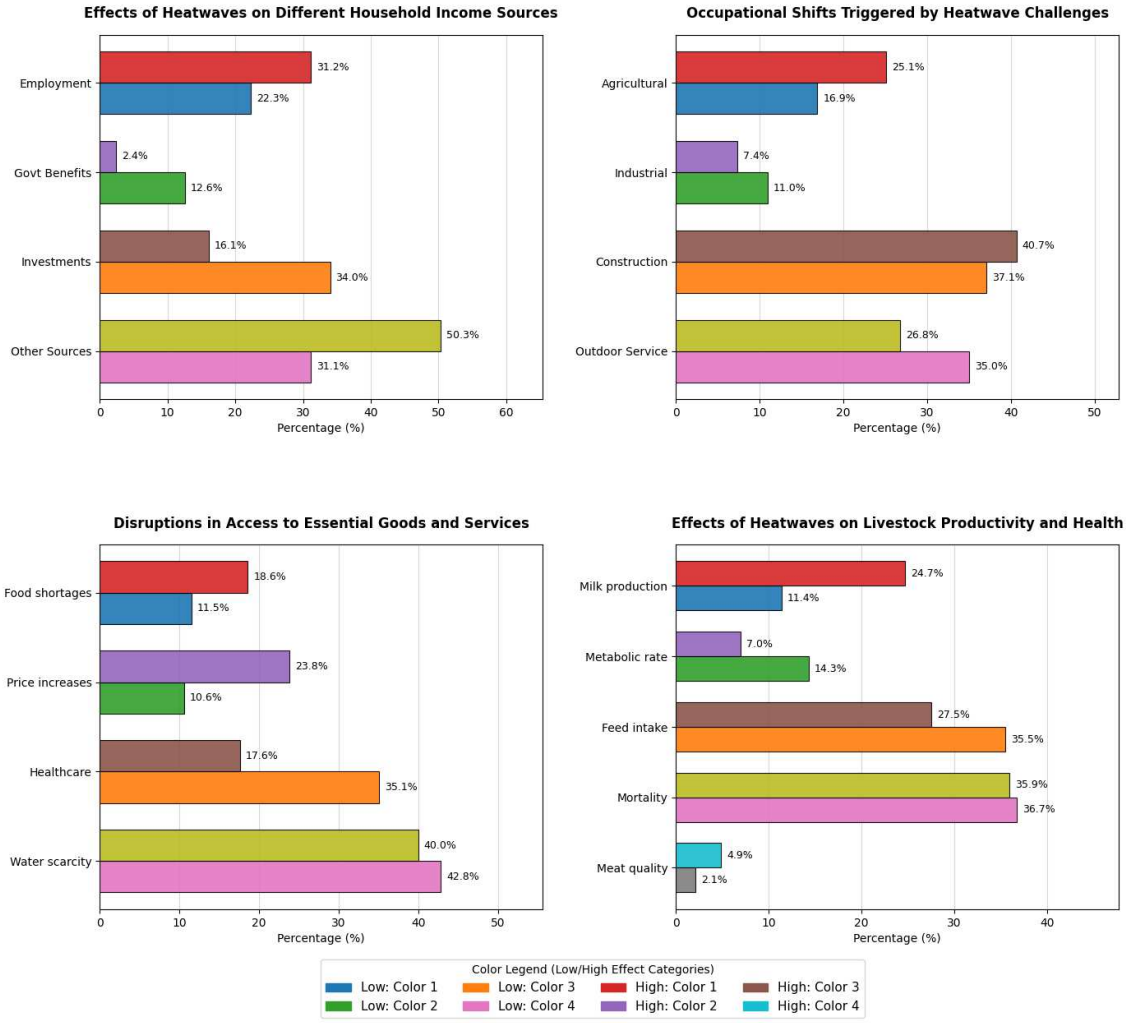


Fig. 20: Heatwave-Induced Livelihood and Service Disruptions in Urban Communities

Figures

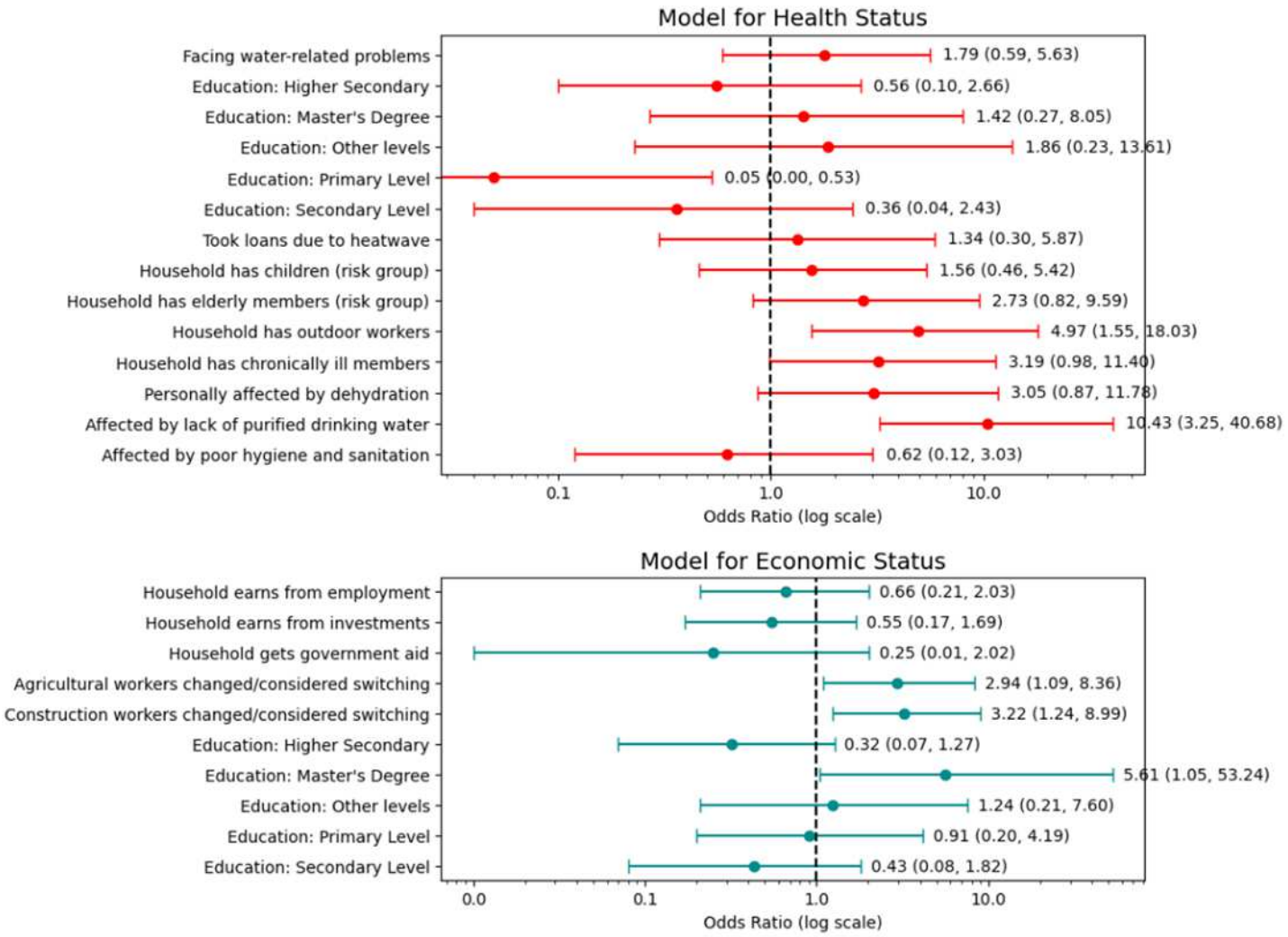


Fig. 21: Determinants of Health and Economic Vulnerability to Heatwaves: Logistic Regression Analysis (Odds Ratios)

Tables

Table 1: Information on Landsat satellite images. Source: US Geological Survey, 2025.

Satellite Type	Data	Sensor	Uses	Path/Row	Cloud Cover %
Landsat 05	January 5, 1995	TM	LULC	137/44	Less than 5 %
	April 2, 1995		LST, UHI		
Landsat 05	March 5, 2005	TM	LULC	137/44	
	April 13, 2005		LST, UHI		
Landsat 08	January 28, 2015	OLI	LULC	137/44	
	April 11, 2016		LST, UHI		
Landsat 08	January 7, 2025	OLI	LULC	137/44	
	April 13, 2025		LST, UHI		

Table 2: Description of land cover categories (Anderson et al., 1976).

LULC Classes	Descriptions
Water Bodies	Areas that are contained by a reservoir, pond, lake, river, or stream.
Vegetation	Lands that are naturally vegetated, coastal mangroves, shrubs, and shrubbery, agricultural lands, including paddy fields, cultivable lands, fruits, and vegetables.
Urban	commercial, residential, industrial, and institutional structures. Together with Transportation/Communications/Utilities, mixed-use developments.
Bare Land and Others	unproductive lands that are devoid of vegetation, trees, or built structures, as well as open lands that are exposed to the soil.

Table 3: Accuracy Assessment of Land Use/Land Cover Classification (1995–2025)

Year	User Accuracy				Producer Accuracy				Overall Accuracy	Kappa Coefficient
	Water body	Urban	Vegetation	Bare land	Water body	Urban	Vegetation	Bare land		
1995	1	0.83	0.9	0.9	1	0.76	0.89	0.96	0.9	0.87
2005	0.88	0.9	0.87	0.86	0.94	0.91	0.91	0.78	0.88	0.84
2015	1	0.89	1	0.92	0.94	0.96	0.96	0.92	0.94	0.93
2025	1	0.95	1	0.92	1	0.92	1	0.96	0.96	0.95

Table 4 (a): Pearson Correlation Matrix for LST, NDBI, NDVI, and UHI in Khulna (year 1995 & 2005)

	Year 1995				Year 2005			
	LST	NDBI	NDVI	UHI	LST	NDBI	NDVI	UHI
LST	1	0.013	0.269	0.992	1	0.708	-0.251	0.986

Tables

NDBI	0.013	1	-0.236	0.038	0.708	1	-0.321	0.712
NDVI	0.269	-0.236	1	0.257	-0.251	-0.321	1	-0.231
UHI	0.992	0.038	0.257	1	0.986	0.712	-0.231	1

Table 4 (b): Pearson Correlation Matrix for LST, NDBI, NDVI, and UHI in Khulna (year 2016 & 2025)

	Year 2016				Year 2025			
	LST	NDBI	NDVI	UHI	LST	NDBI	NDVI	UHI
LST	1	0.771	-0.209	1	1	0.743	-0.143	-0.189
NDBI	0.771	1	-0.328	0.771	0.743	1	-0.191	-0.056
NDVI	-0.209	-0.328	1	-0.209	-0.143	-0.191	1	0.3
UHI	1	0.771	-0.209	1	-0.189	-0.056	0.3	1

Table 5: Regression Analysis (Health and Economy)

Variable	Odds Ratio	Confidence Interval (95%)		P-Value
		Lower Limit	Upper Limit	
Health Model				
Facing water-related problems	1.79	0.59	5.63	$p \geq 0.05$
Education: Higher Secondary	0.56	0.10	2.66	$p \geq 0.05$
Education: Master's Degree	1.42	0.27	8.05	$p \geq 0.05$
Education: Other levels	1.86	0.23	13.61	$p \geq 0.05$
Education: Primary Level	0.05	0.00	0.53	$p < 0.05$
Education: Secondary Level	0.36	0.04	2.43	$p \geq 0.05$
Took loans due to heatwave	1.34	0.30	5.87	$p \geq 0.05$
Household has children (risk group)	1.56	0.46	5.42	$p \geq 0.05$
Household has elderly members (risk group)	2.73	0.82	9.59	$p \geq 0.05$
Household has outdoor workers	4.97	1.55	18.03	$p < 0.01$
Household has chronically ill members	3.19	0.98	11.40	$p \geq 0.05$
Personally affected by dehydration	3.05	0.87	11.78	$p \geq 0.05$
Affected by lack of purified drinking water	10.43	3.25	40.68	$p < 0.001$
Affected by poor hygiene and sanitation	0.62	0.12	3.03	$p \geq 0.05$
Economic Model				
Household earns from employment	0.66	0.21	2.03	$p \geq 0.05$
Household earns from investments	0.55	0.17	1.69	$p \geq 0.05$
Household gets government aid	0.25	0.01	2.02	$p \geq 0.05$

Tables

Variable	Odds Ratio	Confidence Interval (95%)		P-Value
		Lower Limit	Upper Limit	
Agricultural workers changed or considered switching	2.94	1.09	8.36	$p < 0.05$
Construction workers changed or considered switching	3.22	1.24	8.99	$p < 0.05$
Education: Higher Secondary	0.32	0.07	1.27	$p \geq 0.05$
Education: Master's Degree	5.61	1.05	53.24	$p \geq 0.05$
Education: Other levels	1.24	0.21	7.60	$p \geq 0.05$
Education: Primary Level	0.91	0.20	4.19	$p \geq 0.05$
Education: Secondary Level	0.43	0.08	1.82	$p \geq 0.05$

Table 6: Regression Analysis (Health and Economy)

Variable	Category	Odds Ratio	Confidence Interval (95%)		P-Value
			Lower	Upper	
Health Effects					
Facing water-related problems	No issue (Reference)	-	-	-	-
	Water issue	1.29	0.72	2.32	$p > 0.05$
Education	Bachelor's Degree (Reference)	-	-	-	-
	Primary Level	0.02	0.00	0.11	$p < 0.001$
	Secondary Level	0.51	0.16	1.5	$p > 0.05$
	Higher Secondary	1.26	0.55	2.88	$p > 0.05$
	Master's Degree	1.25	0.58	2.74	$p > 0.05$
	Other levels	1.85	0.61	5.46	$p > 0.05$
Took loans due to the heatwave	No loan (Reference)	-	-	-	-
	Took loan	0.93	0.39	2.17	$p > 0.05$
The household has children	No children (Reference)	-	-	-	-
	Has children	1.85	0.98	3.52	$p > 0.05$
	No elderly (Reference)	-	-	-	-

Tables

Variable	Category	Odds Ratio	Confidence Interval (95%)		P-Value
			Lower	Upper	
The household has elderly members	Has elderly	3.46	1.81	6.73	$p < 0.001$
The household has outdoor workers	No outdoor workers (Reference)	-	-	-	-
	Has outdoor workers	5.99	3.17	11.8	$p < 0.001$
The household has chronically ill members	No chronic illness (Reference)	-	-	-	-
	Has chronic illness	1.88	1.01	3.54	$p < 0.05$
Personally affected by dehydration	Not dehydrated (Reference)	-	-	-	-
	Dehydrated	3.9	2.01	7.76	$p < 0.001$
Affected by a lack of purified water	No water issue (Reference)	-	-	-	-
	Affected by water quality	9.75	5.19	19.4	$p < 0.001$
Affected by poor hygiene/sanitation	No hygiene issue (Reference)	-	-	-	-
	Affected by hygiene	0.86	0.37	1.98	$p > 0.05$